

IMPLEMENTATION OF A PAIN GENERATOR CONTROLLED
BY PRESSURE AND FEASIBILITY IN ITS APPLICATIONS
FOR FUNCTIONAL NEAR-INFRARED
SPECTROSCOPY

by

PAMELA A TEBEBI

Presented to the Faculty of the Graduate School of
The University of Texas at Arlington in Partial Fulfillment
of the Requirements
for the Degree of

MASTER OF SCIENCE IN BIOMEDICAL ENGINEERING

THE UNIVERSITY OF TEXAS AT ARLINGTON

May 2011

Copyright © by Pamela Agwa Tebebi

All Rights Reserved

ACKNOWLEDGEMENTS

I would like to acknowledge all the people who assisted in my journey to obtain my master degree. I want to begin by thanking for Almighty God for His guidance and for always putting the right people in my path. I want to thank my father, Elkana A. Tebebi, who has always encouraged me all my endeavors.

I would like to extend gratitude and appreciate to Dr. Liu for her enduring patience, guidance, and encouragement. Dr. Liu always made provisions to see me after hours to discuss my protocol and data as well as to make pertinent recommendations. I want to also thank Sabin Khadka for working with me to validate the Pressure Pain Generator and conduct testing on the subjects. I want to also thank Sabin for his patience and always being available to assist me after work. I want to also thank Pritam Gautam and Lava Banjara for volunteering to be my test subjects for all the preliminary work.

Last but not the least; I want to appreciate Darling Peters for all his personal time spent assisting to build the Pressure Pain Generator. From parts allocation to testing the design in his base, Darling was committed to see this device work.

December 2, 2010

ABSTRACT

IMPLEMENTATION OF A PAIN GENERATOR CONTROLLED BY PRESSURE AND FEASIBILITY IN ITS APPLICATIONS FOR FUNCTIONAL NEAR-INFRARED SPECTROSCOPY

Pamela Tebebi, MS

The University of Texas at Arlington, 2011

Supervising Professor: Hanli Liu

Pain is a sensory and emotional experience as a result of possible or definite tissue damage. The level of pain is subjective to the individual's consciousness of sensory stimuli. Pain stimuli can be noxious (i.e., potentially damaging) or innocuous (i.e., normally not painful). Therefore, pain perception can be based on the degree of the stimuli. Studies have been done using brain imaging modalities to assess pain. Functional Near-infrared spectroscopy (fNIRS) is a noninvasive imaging tool and has been used to study the hemodynamic variations in the brain induced by a variety of activations.

This research was a feasibility study to implement a Pressure Pain Generator (PPG) and test its success in creating controlled pain at an intensity that can be associated with the hemodynamic measures by fNIRS. First, the PPG was built and calibrated, demonstrating its feasibility in creating mechanical pain through pressure-voltage relationship. Second, the calibrated PPG was used with a human subject to rate pain from

low to high level using the visual analog pain scale. The subject could differentiate different degrees of mechanical pain as the voltage was varied. Third, PPG was utilized in conjunction with an fNIRS brain imager to study hemodynamic responses in the prefrontal cortex area when two levels of pain were induced by the PPG. The results of fNIRS were used to correlate the hemodynamic response with the intensity of the pain stimuli. The results revealed significant changes in concentration of oxygenated hemoglobin during post-stimulation in the prefrontal cortex area. It is clear that the PPG can generate well controlled pain stimuli, which can also be evaluated by fNIRS for pain perception. This feasibility study demonstrates a methodology that can be used to understand the hemodynamic response to pain and correlate it to the perception of pain.

TABLE OF CONTENTS

ACKNOWLEDGEMENTS	iii
ABSTRACT	iv
LIST OF ILLUSTRATIONS.....	ix
LIST OF TABLES	x
Chapter	Page
1. INTRODUCTION.....	1
1.1 Motivation	1
1.2 Pain and the Brain.....	1
1.3 Imaging Assessment of Pain.....	2
1.3.1 Pain Study and fMRI	2
1.3.2 Pain Study and NIRS	3
1.3.3 NIRS and Other Applications	4
1.4 Aim of Study	4
2. METHODS AND MATERIALS	5
2.1 Pressure Pain Generator	5
2.1.1 How Device was Constructed	7
2.1.2 Operation	8
2.1.3 Pressure Pain Generator Glossary	11
2.1.4 Deriving Calibration Curve	11
2.1.5 Stimulus Protocol	11
2.2 CW-6 fNIRS.....	14
2.2.1 Principle	14
2.2.2 Setup and Parameters	14

2.2.3 Functional Role in Stimulus Protocol	15
2.2.4 Data Analysis	16
2.3 Subject	16
2.3.1 Volunteers	16
2.3.2 Subject Testing	17
2.3.3 Testing Setup	17
3. RESULTS	18
3.1 Pressure Pain Generator Design and Protocol Setup	18
3.2 Calibration Curve	21
3.3 Implementation of Pressure Pain Generator and use of NIRS for Human Study	23
3.3.1 Subject's Pain Threshold and Corresponding Voltage	23
3.3.2 Temporal Changes in Oxygenated Hemoglobin Concentration due to Pain Stimulation	24
3.3.3 Graphical Comparison of Change in Oxygenated Hemoglobin Concentration over Time	28
3.3.4 Spatial Profile of Change in Oxygenated Hemoglobin Concentration over Time	40
4. DISCUSSION AND CONCLUSION	32
4.1 Discussion	32
4.2 Conclusion	34
4.3 Future Work	35
APPENDIX	
A. RAW DATA OF CHANNELS WITH CORRESPONDING TEMPORAL AND SPATIAL PROFILES AT DIFFERENT TIME SEGMENTS	36
B. RAW DATA OF COMPARING CHANGE IN OXYGENATED HEMOGLOBIN AT EACH CHANNEL	46
REFERENCES	54

BIOGRAPHICAL INFORMATION57

LIST OF ILLUSTRATIONS

Figure	Page
2.1 Pain generating apparatus created by Kohlloffel et al [17].	6
2.2 Major Components of Pressure Pain Generator	8
2.3 Pressure Pain Generator.	10
2.4 Threshold Stimulus Protocol	12
2.5 Visual Analog Pain Scale [20]	12
2.6 Stimulus protocol using 30% and 60% of threshold for Pain Level 3 and 6	13
2.7 fNIRS instrument - CW-6 [13]	14
2.8 Source-Detector Pair Configuration	15
2.9 Light path of source-detector pair [22]	16
2.10 Subject's hand positioned under brass cylinder at the point of mechanical impact and CW source detector probes assembled around forehead	17
3.1 Pressure Pain Generator	19
3.2 System Setup	20
3.3 Pressure Voltage relationship derived from the E/P Transducer	22
3.4 Configuration of source-detector pairs (channels)	25
3.5 Source 2 - Channel configuration (a), corresponding temporal (b) and spatial (c) plots of subject with a pain level of 3.	27
3.6 Averaged changes in HbO at each channel over the 5-sec Baseline (blue bars) and 5-15 seconds post stimulation (red bars), with pressure stimulation of pain level 3; Error bars: the standard deviation	29
3.7 Spatial profile of pain level 3 and level 6 over time.....	31
A.1 Source 1 - Channel configuration (a), corresponding temporal (b) and spatial (c) plots of subject with a pain level of 3.....	38

A.2 Source 2 - Channel configuration (a), corresponding temporal (b) and spatial (c) plots of subject with a pain level of 3.....	39
A.3 Source 3 - Channel configuration (a), corresponding temporal (b) and spatial (c) plots of subject with a pain level of 3.....	40
A.4 Source 4 - Channel configuration (a), corresponding temporal (b) and spatial (c) plots of subject with a pain level of 3.....	41
A.5 Source 1 - Channel configuration (a), corresponding temporal (b) and spatial (c) plots of subject with a pain level of 6.....	42
A.6 Source 2 - Channel configuration (a), corresponding temporal (b) and spatial (c) plots of subject with a pain level of 6.....	43
A.7 Source 3 - Channel configuration (a), corresponding temporal (b) and spatial (c) plots of subject with a pain level of 6.....	44
A.8 Source 4 - Channel configuration (a), corresponding temporal (b) and spatial (c) plots of subject with a pain level of 6.....	45
B.1 Mean of the change in deoxygenated hemoglobin at each channel over -5 to 0 seconds	48
B.2 Mean of the change in deoxygenated hemoglobin at each channel over 0 to 5 seconds.....	48
B.3 Mean of the change in deoxygenated hemoglobin at each channel over 5 to 15 seconds.....	49
B.4 Mean of the change in deoxygenated hemoglobin at each channel over 15 to 30 seconds	49
B.5 Mean of the change in deoxygenated hemoglobin at each channel over 30 to 40seconds.....	50
B.6 Mean of the change in deoxygenated hemoglobin at each channel over -5 to 0 seconds.....	51
B.7 Mean of the change in deoxygenated hemoglobin at each channel over 0 to 5 seconds.....	51
B.8 Mean of the change in deoxygenated hemoglobin at each channel over 5 to 15 seconds.....	52
B.9 Mean of the change in deoxygenated hemoglobin at each channel over 15 to 30 seconds.....	52
B.10 Mean of the change in deoxygenated hemoglobin at each channel over 30 to 40 seconds.....	53

LIST OF TABLES

Table	Page
3.1 Subject pain threshold rating data and corresponding pain scale	24

CHAPTER 1

INTRODUCTION

1.1 Motivation

The most common cause for medical appointments in the USA is pain in addition to the adverse effects on the quality of life such as eating, sleeping, cognition, and functional status [1]. The Annual NIH Pain Consortium Symposia has emphasized the need for research that can lead to preventive and effective treatment of unwanted pain. Treatment development for acute and chronic pain requires understanding of the process underlying the transmission and perception of pain stimuli. Progress had been made in the identification of the neural pathways of pain; however, the experience of pain and its treatment are often a mystery. In addition, there is a need to quantify pain and to assess the neural response of pain such that appropriate treatments can be administered more effectively.

1.2 Pain and the Brain

Pain is a complex term to define. According to the International Association for the Study of Pain (IASP), pain is a sensory and emotional experience as a result of possible or definite tissues damage [2]. Tiengo and others define pain as an individual's consciousness of the nociceptive message [2,3]. When someone has been aware by his or her cognitive sense that he or she is in pain, then that person can say he or she is experiencing pain. Nociceptive pain is a result of the stimulation of peripheral nerve fiber beyond its threshold such that nociceptors (sensory receptors) are activated, sending signals from the site of activation through the spinal cord to the brain [1,2,3]. This process is called nociception, and it's the cause of the perception of pain [1,2,3].

Perception of pain is subjective, therefore making it difficult to quantitatively measure pain clinically [3]. In addition, the mental stages will affect the perceived pain due to the fact that the integration of nociceptive signals is affected by other underlying neural events. According to Tiengo et al [2], modulating the integration of the nociceptive signals can enhance or reduce pain perception. The

three major types of nociceptors that can be modulated are thermal, mechanical, and polymodal [3]. Thermal nociceptors are triggered by extreme temperature, mechanical nociceptors are triggered by concentrated pressure to the skin, and polymodal nociceptors can be triggered by high-intensity mechanical, chemical or thermal stimuli [3]. Stimuli can be noxious (strong, potentially damaging) or innocuous (weak, normally not painful) [3]. Therefore, pain perception can be based on the degree of the stimuli. Lopes-Sola et al [10] commented on the fact that the frontal cortex is an interesting area to image pain experience because its function for cognitive and emotional processing, based on research done by others.

1.3 Imaging Assessment of Pain

Several neuroimaging studies have been done to investigate which brain regions are active in response to pain and to understand the neural activities associated with pain stimulation. Some of these imaging techniques include fMRI, EEG/MEG, PET/SPECT, MR spectroscopy, and near infrared spectroscopy (NIRS). Apkarian et al [8] did a literature review, examining the imaging techniques and their abilities to map different pain states. From the review, fMRI and NIRS methods utilize hemodynamic features as the key parameters for the of measurement.

1.3.1 Pain Study and fMRI

In assessing pain, several modalities are currently being used. One common modality is functional magnetic resonance imaging (fMRI), which is blood-oxygenation-level dependent (BOLD) [4]. BOLD signals measure relative changes induced by brain stimulations as a function of changes in deoxygenated hemoglobin (HbR) concentration [4]. Neural activation as a consequence of brain stimuli results in an increase in blood flow and thus an influx of oxygenated hemoglobin (HbO) as well as a reduction of deoxygenated hemoglobin [4,5]. In principle, BOLD signals reflect the changes in cerebral blood flow, cerebral metabolic rate of oxygen, and cerebral blood volume, all of which are referred to as the hemodynamic response to activation [4,5,6]. BOLD fMRI makes it easier to study the physiological processes in the brain through the output measure of the hemodynamic response.

A study by Andrea et al [7] and Stammer et al [9] confirmed cortical areas activated by mechanical pain and touch stimuli. Activation was present in the pain matrix, which consisted of somatosensory projection, cingulate gyrus, anterior insula, premotor areas, prefrontal, and posterior parietal areas [7,9]. In another study, using fMRI to understand brain mechanism of pain perception, slight activation was present during the anticipatory cue and magnified during pain stimulus; it confirmed that this imaging modality (i.e., fMRI) is useful to understand the network of pain perception [8]. Lopes-Sola et al [10] demonstrated the presence of anticipatory activation and increased activation during pain stimulation; however, when the stimulus was removed, the activation gradually decreased. Lui et al. [21] used fMRI to study mechanical stimulus anticipation, perception, and coding; they showed consistent results with other studies that reported increased fMRI signals in the parietal, insular, frontal and cingulate cortical regions, following brief mechanical stimuli, while displaying decreased BOLD signals in the medial prefrontal cortex and elsewhere.

1.3.2 Pain Study and NIRS

Near-infrared spectroscopy (NIRS) is a noninvasive imaging tool that takes advantage of the absorption spectral relationship between water, oxygenated hemoglobin, and deoxygenated hemoglobin [11,13]. Functional NIRS (fNIRS) has been used to study the hemodynamic variations in the brain induced by activation [19]. In principle, near-infrared light penetrates the scalp, skull, and brain, and then it reflects back to a light detector. The detected light intensity varies based on the hemodynamics of neural activation [11]. To meet the energy demands of neural activation in the brain, there is an increase in cerebral blood flow to the site. The neural stimulation results in an elevation of the local concentration of oxygenated hemoglobin and a decrease in deoxygenated hemoglobin, following the same physiological principle as explained for BOLD signals. As an example, Bartocci et al. [14] have elicited hemodynamic responses due to painful and tactile stimulation in the somatosensory cortex in studying pain processing in neonates.

1.3.3 NIRS and Other Applications

NIRS with its portability and minimal susceptibility to motion artifacts has been used in a variety of applications. Tachtsidis [15] et al. used NIRS to show frontal cortex activation as a result of solving anagrams. Bortfeld et al [11] used NIRS to study the cortical response of infants with speech as the stimuli and concluded that NIRS is a feasible tool for tracking neural activity as well as studying perception and cognition. Sitaram et al [12] tested the potential of using NIRS to access neural activity in development of a brain-computer interface. Tian et al [18] incorporated fNIRS to show nonlinearity of the hemodynamic responses in the prefrontal cortex when subjects performed anagram tasks; in another study [19], they reported the association between the hemodynamic response and neuronal activity of deception.

1.4 Aim of Study

This research was a feasibility study to implement and test a pressure-controlled pain generator, as well as to demonstrate its success in creating controlled pain at variable pain intensity. Specifically, the aim of the current study is to build a device that can induce controlled mechanical pain, which can be correlated with hemodynamic responses measured in the prefrontal cortex through the use of near-infrared spectroscopy. There are two parts to meet this objective. The goals of part I were: 1) to design a controlled pain stimulation apparatus, 2) to quantify the pain thresholds by a voltage-pressure relationship, and 3) to correlate pain levels (controlled by pressure) with subjects' rating of pain. The goal of part II was to successfully create mechanical pain while simultaneously record the corresponding hemodynamic signals on the subject's forehead. To achieve this goal, the newly implemented pressure-controlled-pain generator and a fNIRS brain imaging system (TechEn, CW 6) were employed.

CHAPTER 2

METHODS AND MATERIALS

2.1 Pressure Pain Generator

This study aimed to examine the feasibility of a pain-inducing system via pressure that can be used to show a correlation between controlled mechanical pain stimulus and the corresponding hemodynamic signals in response to pain. It necessitated a system that can deliver consistent and controlled pain stimuli to the skin such that the hemodynamic response in the brain can be detected and evaluated. It was critical that controlled mechanical stimuli could be reproduced among subjects. The pressure-controlled pain generator is based on a technique developed by Kohlloffel et al. [16] to evaluate mechanical pain and hyperalgesia, the exaggerated sense of pain. The apparatus (see Figure 2.1) pneumatically accelerates an aluminum cylinder to the skin through a barrel to create innocuous or noxious pain. The technique by Kohlloffel et al [16] offered a method to vary and reproduce pain levels; it is a feasible approach to quantify stimulating levels of pain.

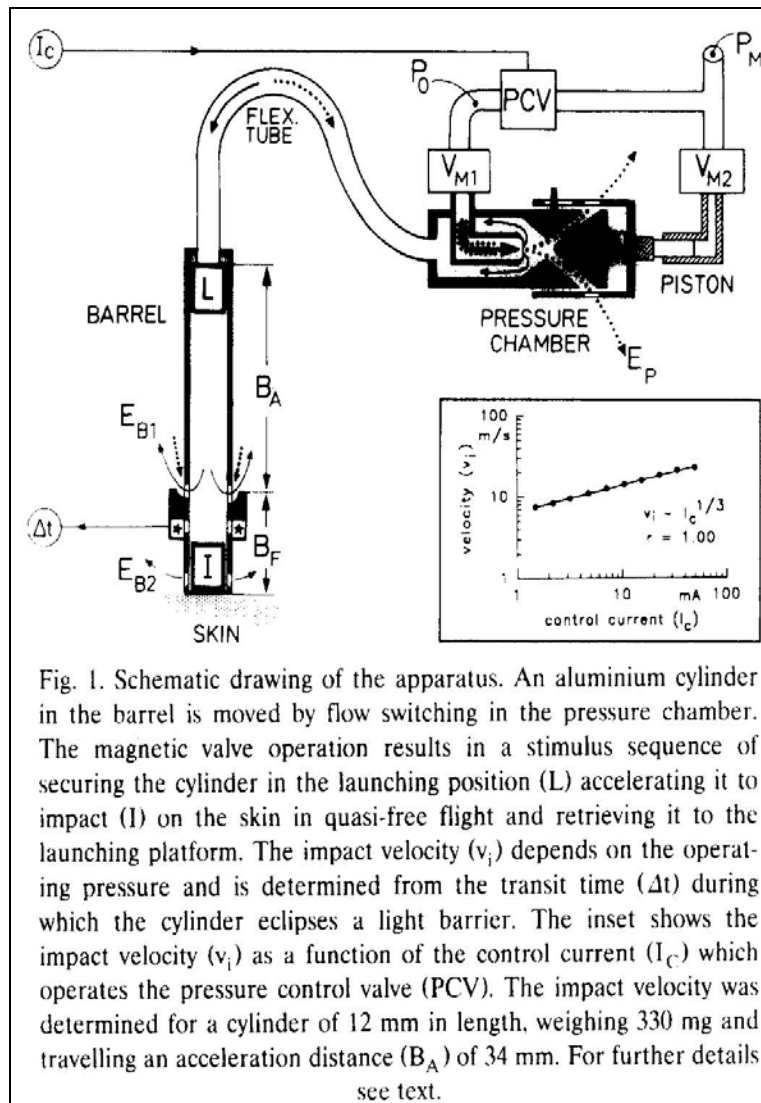


Figure 2.1 Pain-generating apparatus created by Kohlloffel et al [17].

Koltzenburg et al [17] took advantage of Kohlloffel's technique to correlate action potential resulting from the mechanical stimulation of nociceptor with the associated vasodilation. Psychophysical measures showed that the magnitude of pain was dependent on the frequency of the mechanical stimulation. Schoedel et al. [7] also used Kohelloffel's technique to understand how the rating of painful and non-painful mechanically stimulated pain influenced hemodynamic responses recorded in fMRI. More cortical regions were activated during the rating of sensory task when compared to the regions activated when rating was not being performed.

2.1.1. How Device was Constructed

In my study, the Pressure Pain Generator (PPG) was built from various components ranging from scrapped parts to new parts. I applied the concept developed by Kohelloffell et al [17] but built the device using different components. Figure 2.2 shows all major components that I used to build my PPG. The following list is the constructional overview of the components needed for the device. Verification was done after each step to ensure each component's functionality:

1. Air accumulator separated by a welder;
2. Valve used from a blood analyzer was located, removed, and its functionality assessed;
3. Airflow single valve was installed to a wooden frame with a respective 12-V power supply;
4. Air lines installed to the respective points and checked for successful air flow;
5. Brass cylinder acquired and target sized accordingly;
6. E/I Transducer and corresponding power supply installed and verification of operability checked according to manufacturer specification;
7. Compressor and vacuum installed and testing performed.

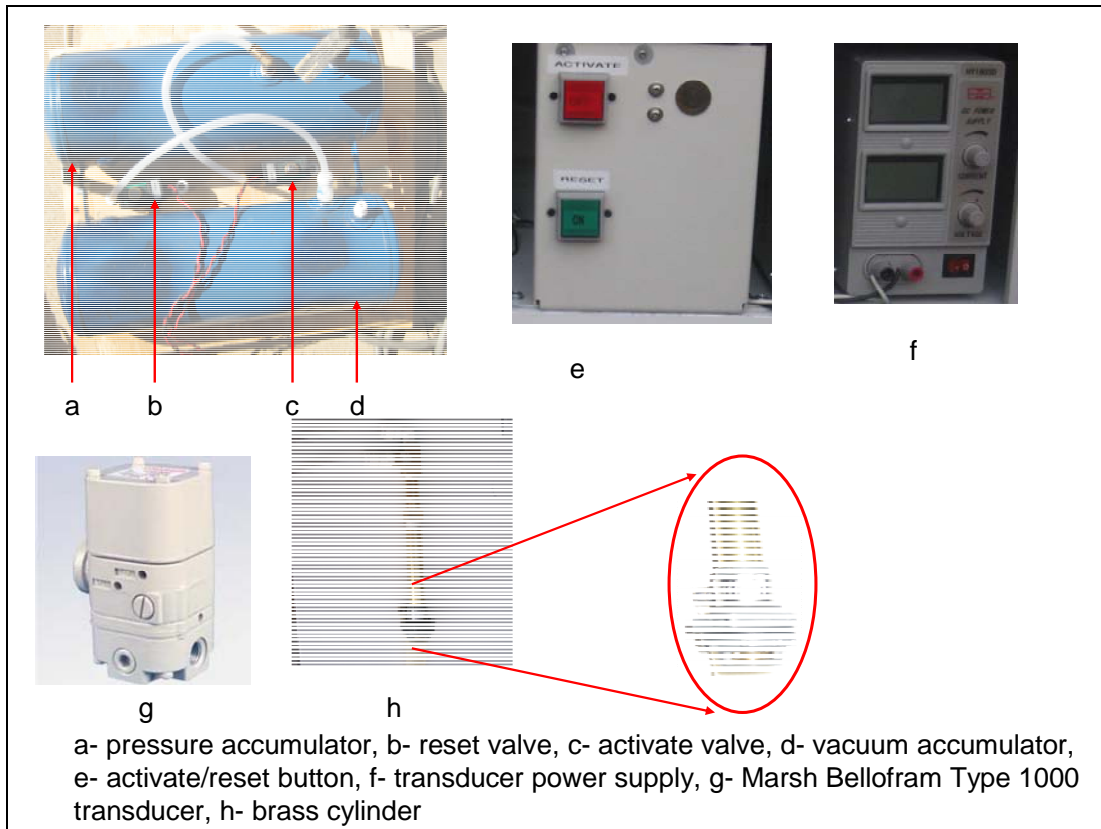


Figure 1.2 Major Components used for Pressure Pain Generator

2.1.2. Operation

The purpose of implementing the pressure pain generating device is to provide different levels of pain through a controlled pressure. Figure 2.3 is the block diagram of the apparatus. Pressure is used to propel the target to the forearm of the subject while vacuum is used to withdraw the target back to the starting point. To perform this task, a compressor is needed to create a supply pressure between 125 and 150 psi, which is the required specification for the pressure/voltage transducer. The pressurized air is fed into a pressure accumulator. From the pressure accumulator, the pressurized air is routed to the pressure/voltage transducer, which correlates a voltage to a pressure. There are two pressure gauges used in the device: one on the incoming line of the transducer so as to monitor the supply pressure, and another one on the transducer to monitor the output pressure that was used to propel the target. To set the required output pressure, an input voltage is set through a DC voltage-controlled power supply. Once

the voltage is set, the ball valve must be closed, so only a negligible amount of air is lost to the vacuum line before the activation button is pressed. Once the button is pressed, the normally closed valve 1 is opened to release air to propel the target toward the forearm at the corresponding pressure. The aluminum target travels approximately 144 mm down a hollow brass cylinder to create an impact on the forearm. The target is approximately 12 mm in diameter by 16.5 mm in lengths with a mass of approximately 4.69 g. To retract the target back to the starting point of the brass cylinder, the 2nd ball valve must be open so that when the reset button is pressed, the normally closed valve 2 opens and vacuum pulls up the target back to the starting point. To propel the target at different pressures, the corresponding voltages are set on the DC power supply, and the entire process is repeated.

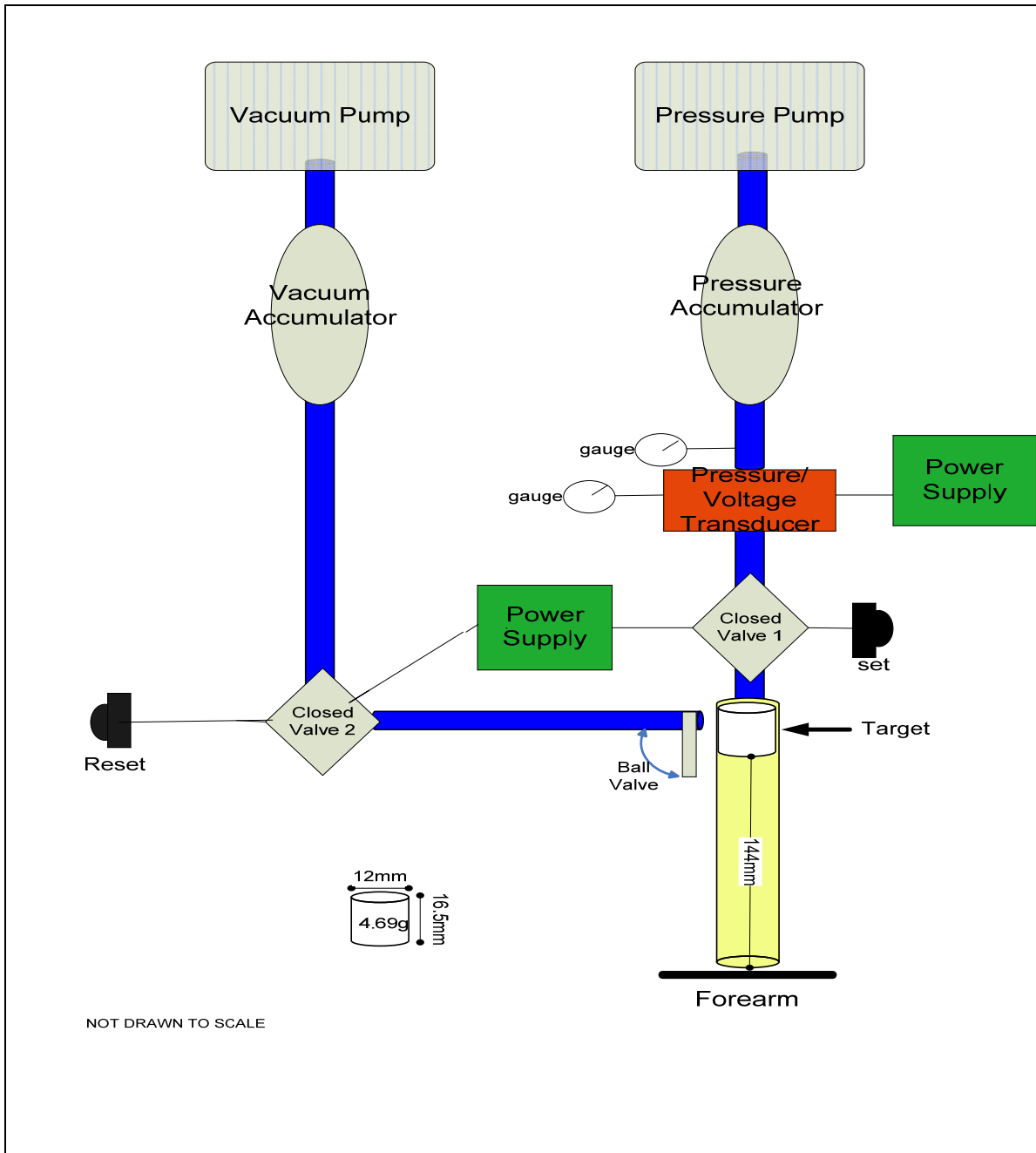


Figure 2.3 Block diagram of Pressure Pain Generator.

2.1.3. Pressure Pain Generator Glossary

1. Pressure Pump: a compressor used to generate a supply pressure between 125-150 psi for the transducer;
2. Vacuum Pump: used as the vacuum source;
3. Vacuum Accumulator: used to house necessary air volume;
4. Pressure Accumulator: used to house necessary air volume;
5. E/P Transducer: a Marsh Bellofram Type 1000 transducer, 961-112-000, 0-10 V, 3-120 psi;
6. Power Supply (18V): a DC-regulated power supply for the E/P Transducer;
7. Power Supply (12V): a DC power supply used to power the closed valves;
8. Closed Valve 1: open upon pressing the activation button to propel the target to forearm;
9. Closed Valve 2: open upon pressing the reset button to retract the target to the starting point;
10. Target: an aluminum cylinder with a mass of 4.69 g and dimensions of 12 mm X 16.5 mm;
11. Brass Cylinder: air channel used to propel the target to the arm with a length of 144 mm.

2.1.4. Deriving Pressure-Voltage Calibration Curve

The pressure-voltage calibration curve was derived in two ways to check for consistency and linearity of the pressure voltage transducer. One way was to adjust the pressure and then record the corresponding voltage, while the other was to adjust the voltage and record the corresponding pressure. The first way began with a starting point at 4 psi and incremented the pressure by 2 psi while simultaneously recording the corresponding voltage. The second way was done by starting at 0.6 V and incrementing by 0.2 V and recording the corresponding pressure.

2.1.5. Stimulus Protocol

The initial session of stimulation was used to determine a subject's pain threshold. The threshold of each subject was generated by starting at the defined baseline of 0.6 V and incrementing the voltage by 0.2 V until the subject could no longer tolerate the pain induced by the impact of the aluminum target (see Figure 2.4).

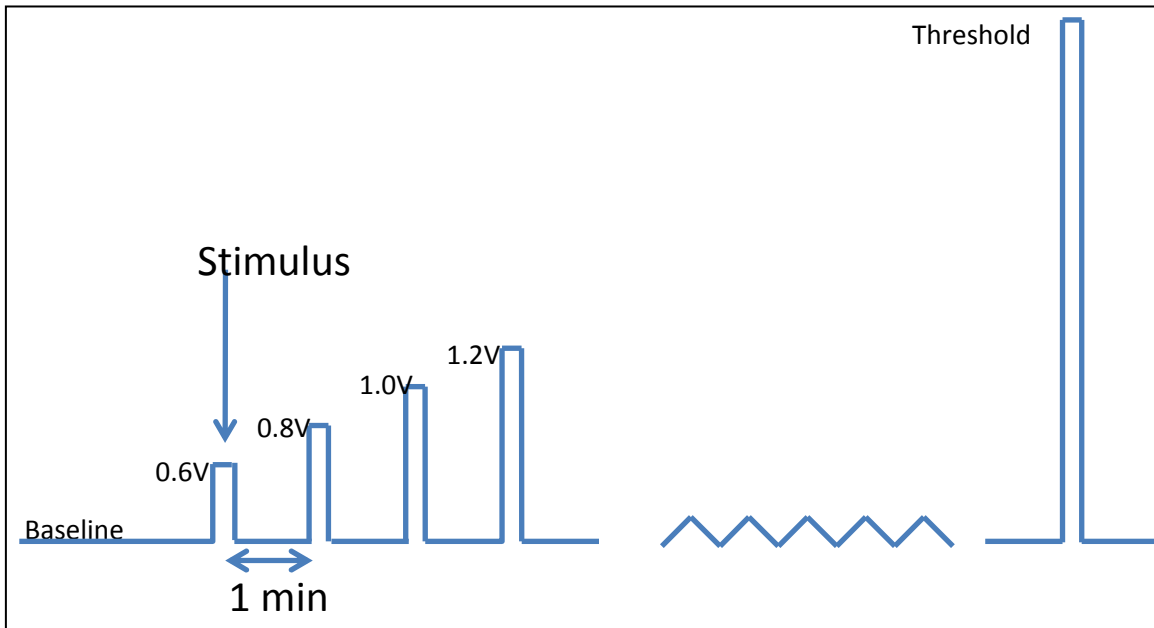


Figure 2.4 Threshold Stimulus Protocol.

The inter-stimulus time was set to be 1 minute. During the stimulation, the subject was asked to rate the intensity of pain by using the Visual Analog Pain Scale [20], as given in Fig. 2.5.

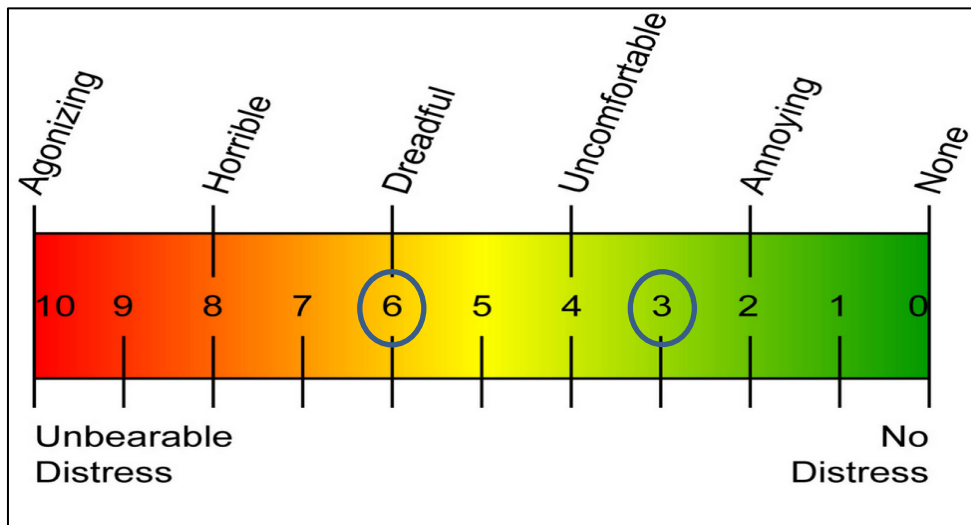


Figure 2.5 Visual Analog Pain Scale [20].

Once the subject reached his or her respective Agonizing pain level, the respective pain threshold had been reached. After the threshold is identified, repetitive stimulations were given at 30% and 60% of the subject's pain threshold. The 30% and 60% of the threshold corresponded to specific voltage levels

on the PPG at which the subject indicated. Averagely, the 30% of the threshold corresponded to pain level of 3 and 60% to pain level 6 on the Visual Analog Pain Scale.

During the measurement, baseline readings were set for 40 seconds prior to the first instance of mechanical stimulation. The mechanical stimulation was given within a 4-sec period with two intervals of pain stimulation. This session of stimulation followed the stimulus protocol, as shown in Figure 2.6, while a simultaneous fNIRS measurement was taken to record the brain activities. Specifically, in Figure 2.6, 'set' corresponds to the step of propelling the target to the skin using pressure, while 'reset' corresponds to pull the target away from the skin back to the origin with vacuum.

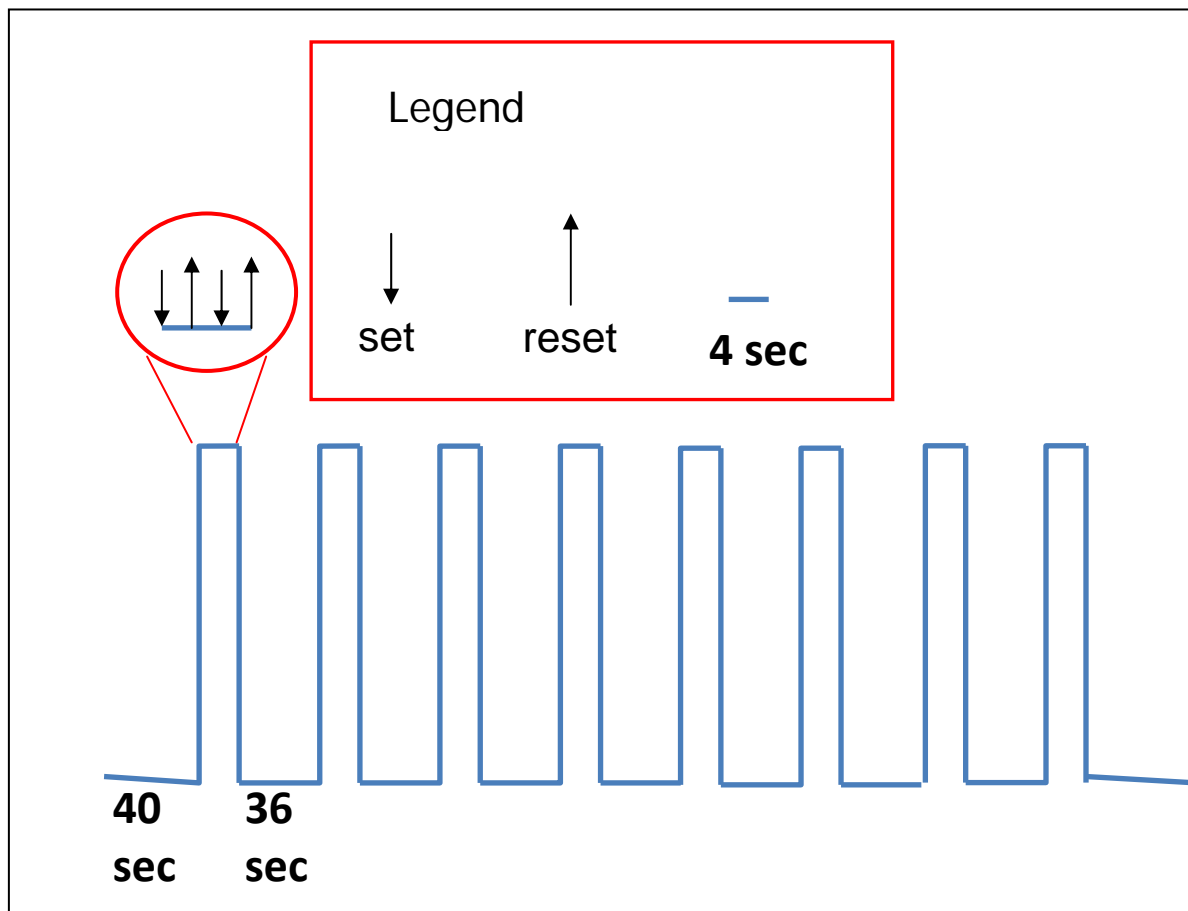


Figure 2.6 Stimulus protocol using 30% and 60% of the threshold for Pain Level 3 and 6.

2.2 CW-6 fNIRS

2.2.1. Background of CW-6

CW-6 made by TechEn is a continuous-wave, imaging system using NIRS to image brain activity in real time [13]. The technology incorporates the absorption properties of water, oxygenated hemoglobin (HbO), deoxygenated hemoglobin (HbR) in tissue to reconstruct spatial variations during brain activities [13]. The system uses laser sources and detectors, interfacing on a control card with a computer. Figure 2.7 shows the front panel of a CW-6 system, which has 32 sources by 32 lasers.

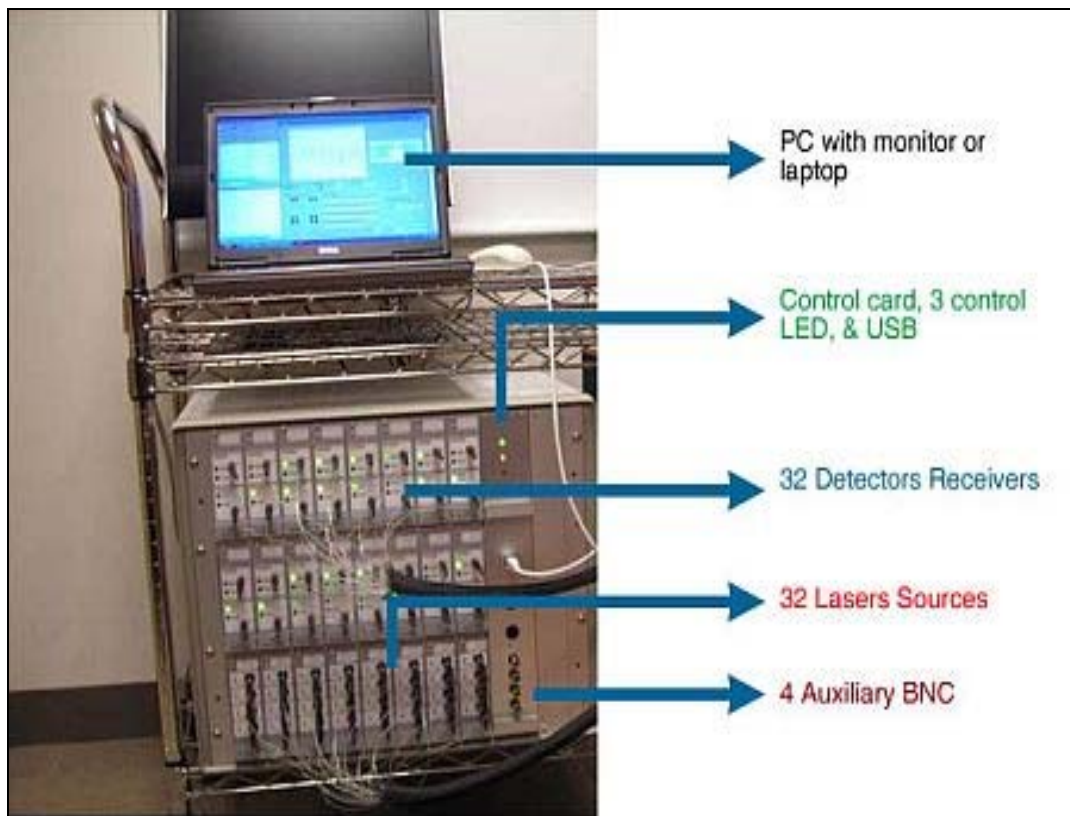


Figure 2.7 fNIRS instrument: CW-6 [13].

2.2.2. Setup and Parameters

The CW-6 NIRS system used in the study consisted of 4 pairs of laser diodes as light sources emitting at wavelengths of 690 nm and 830 nm and 20 detectors. The symmetrical arrangement of the

fiber probes is seen in Figure 2.8. The fiber probe array was placed across the subject's forehead; there were 22 source-detector pairs (channels) with a source-detector separation of 2.5 cm. During scanning, Velcro band was used to secure the probes to the forehead (Fig. 2.8).

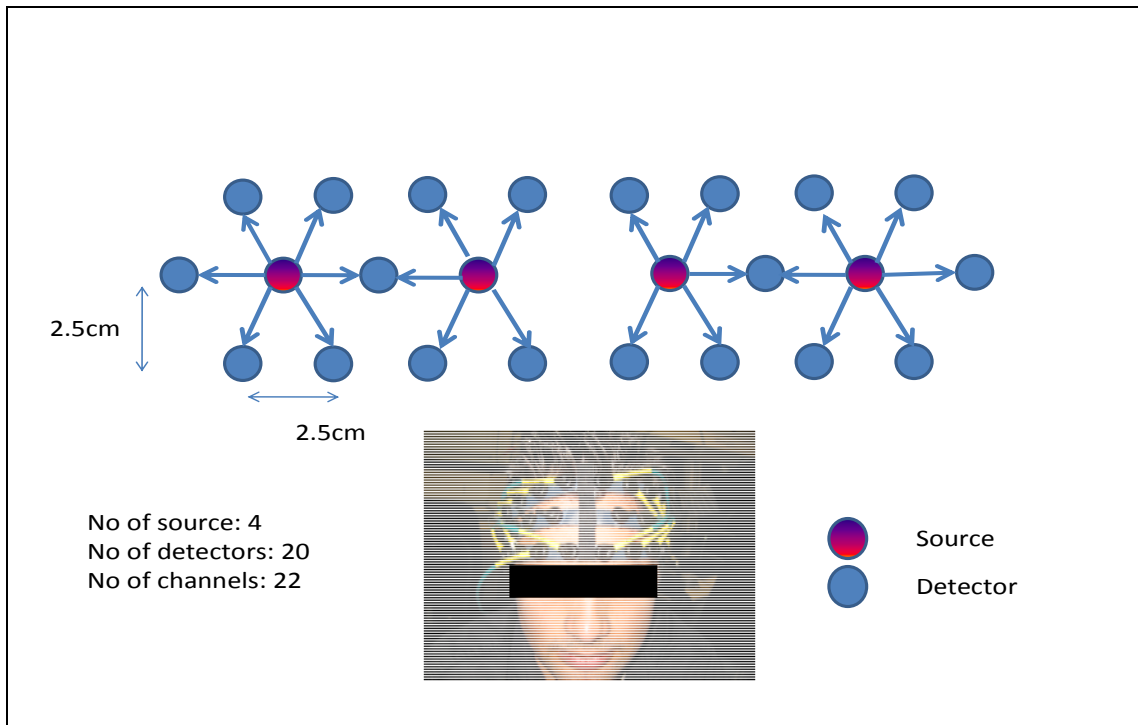


Figure 2.8 Source-Detector Pair Configuration.

2.2.3. Functional Role in Stimulus Protocol

The NIRS probes were taking readings when the pain stimulus protocol at 30% and 60% of the pain threshold were initiated. The diffused NIR light penetrated the scalp, and the nearest detectors recorded the reflected light from the brain (Figure 2.9). The recorded signals allow us to determine changes in oxygenated hemoglobin concentrations as a function of time and locations, so both temporal profiles and 2-dimensional spatial maps can be generated.

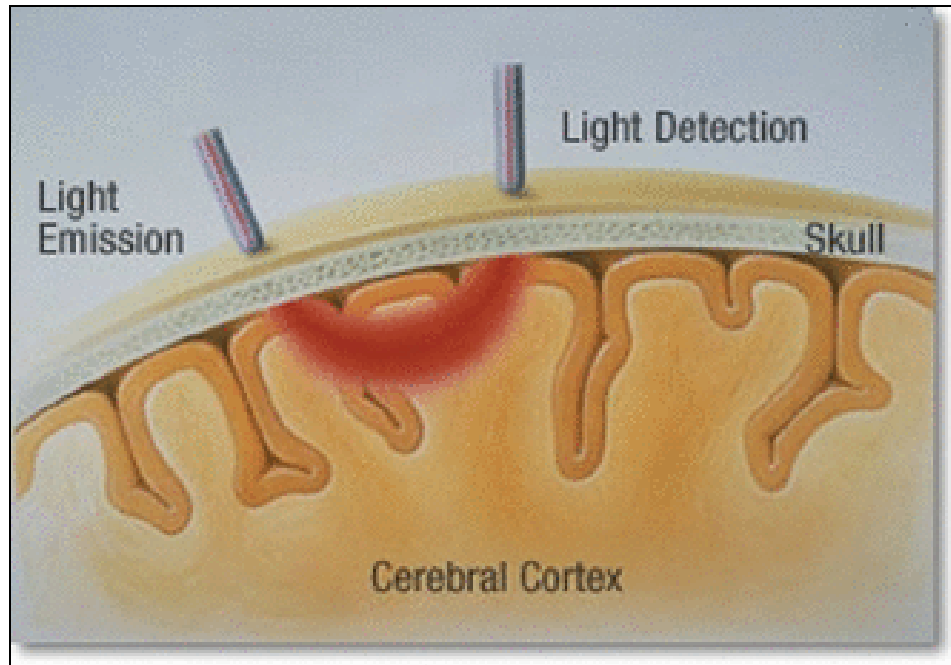


Figure 2.9 Light path of source-detector pair [22].

2.2.4. Data Analysis

Functional NIRS data analysis was done using HomER [23], which is a free software developed by Photon Migration Imaging lab at Massachusetts General Hospital. HomER is a tool used for filtering, analysis, and image reconstruction of NIRS data to further understand hemodynamic responses of the brain to functional stimulations [23]. Data analysis was performed for each subject on a channel by channel basis. To remove any baseline drift, a high pass filter of 0.03 Hz was applied; to remove any physiological artifacts, such as the heart pulsation, a low pass filter of 0.3 Hz was applied. The processed signals resulted in changes in HbO concentration, averaged over 8 blocks with each block being 40 seconds in duration; corresponding reconstructed images were also obtained.

2.3 Subject

2.3.1 Volunteer

One subject was used in this feasibility study. The subject was a graduate student who volunteered to test the design and implementation of the pressure pain generator and the study protocol.

2.3.2 Subject Testing

The subject was comfortably seated near a laboratory bench where the brass cylinder was mounted. The subject's hand was positioned such that the volar forearm was underneath the tip of the brass cylinder (Figure 2.10). The aluminum target was propelled approximately 90-100 mm away from the elbow joint.

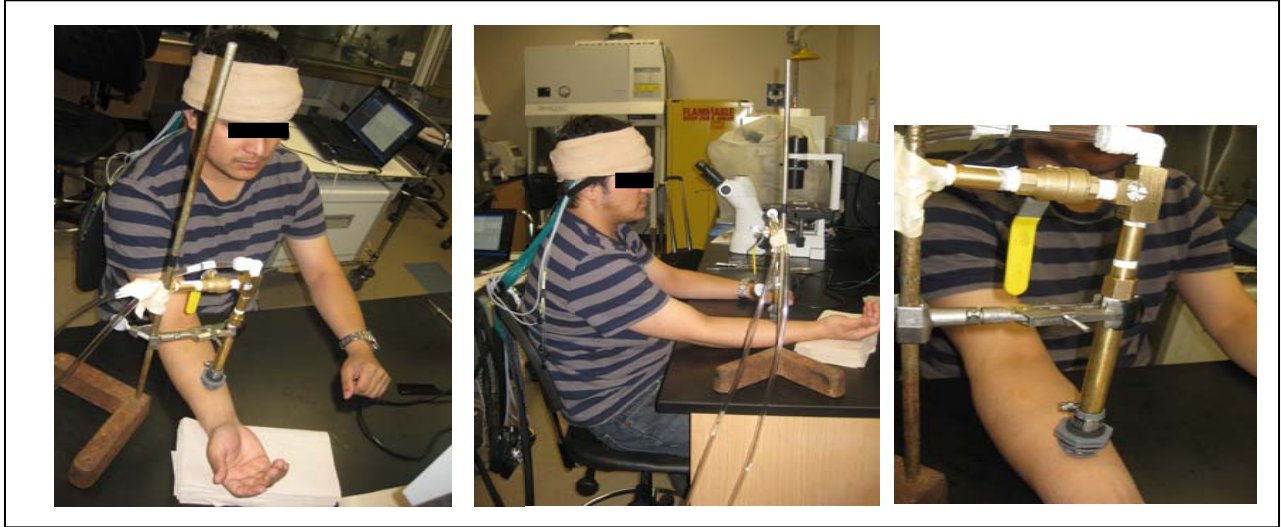


Figure 2.10 Subject's hand was positioned under the brass cylinder at the point of mechanical impact; the CW-6 source-detector probe array was placed around the subject's forehead.

2.3.3 Testing setup

The pain threshold of the subject was determined without monitoring the hemodynamic response. However, the blocked design at both 30% and 60% of the threshold was performed with the NIRS probes attached to the prefrontal cortical area of the subject. The two pain levels were tested on the same day with a 10-minute break between them. Baseline data was collected over several minutes from the same subject on a different day while the subject remained relaxed in a quiet environment with minimal external distraction.

CHAPTER 3

RESULTS

3.1 Pressure Pain Generator Design and Protocol Setup

The Pain Pressure Generator was developed (Figure 3.1) for the study of controlled pain through pressure. The device was designed to function in conjunction with a fNIRS system (CW-6) to understand the relation between pain and corresponding hemodynamic responses (Figure 3.2).

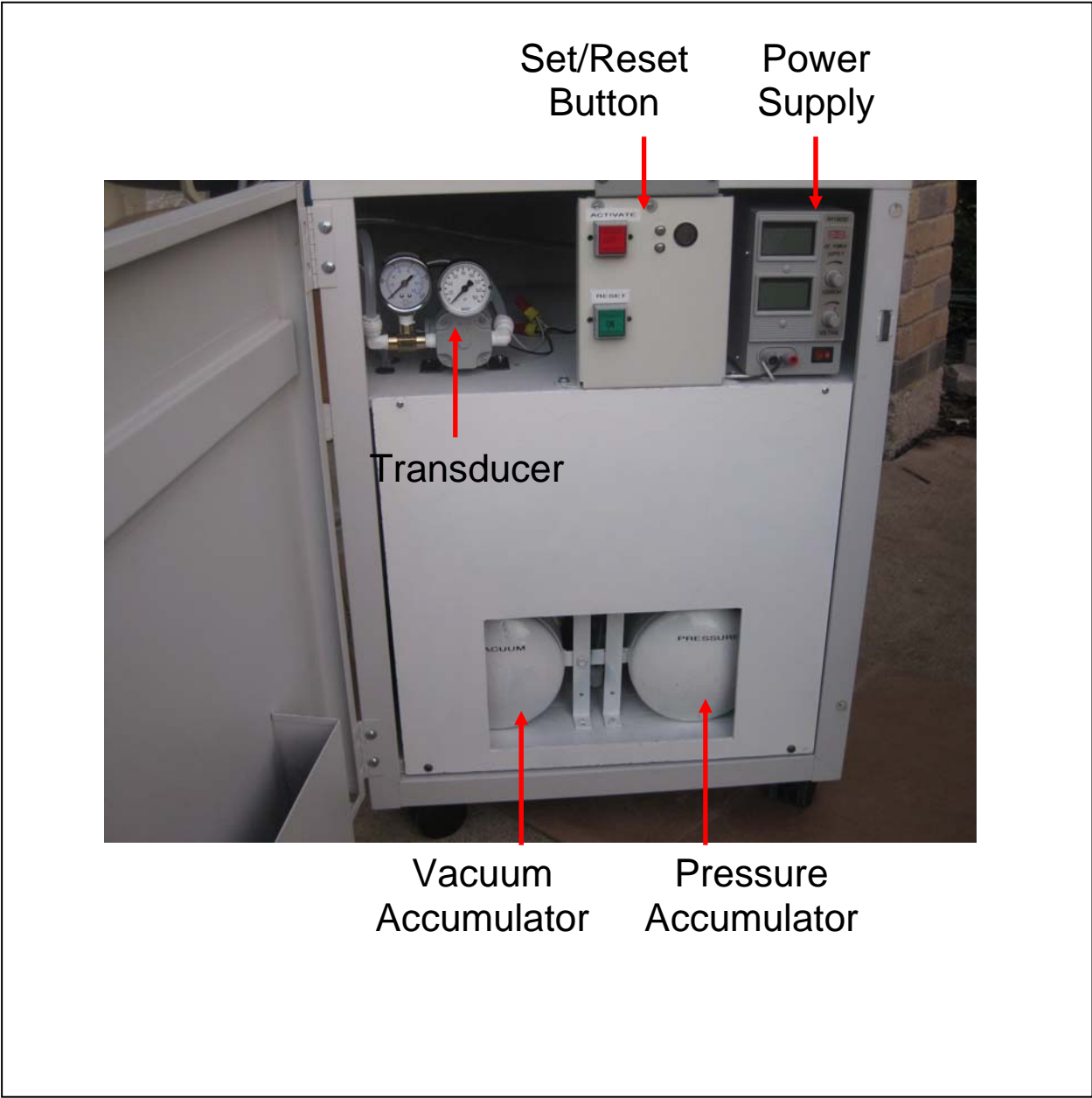


Figure 3.1 Pressure Pain Generator

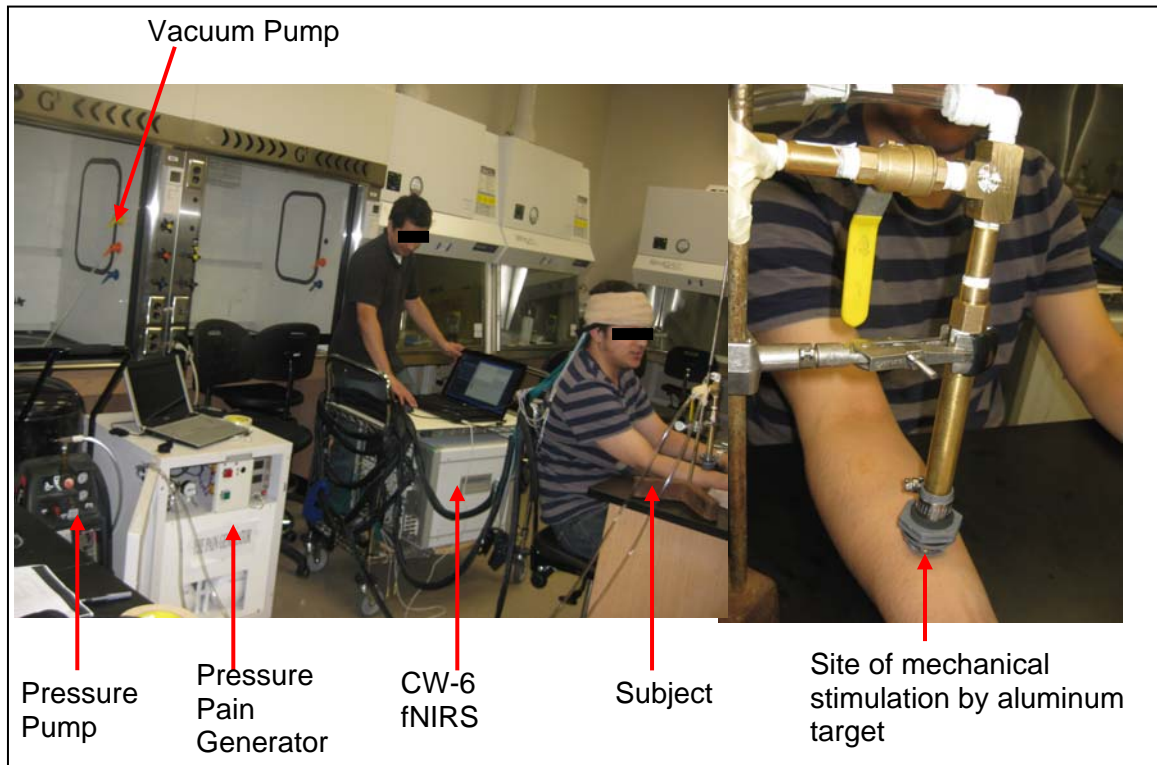


Figure 3.2 System Setup

The protocol to create controlled pain was performed with the assistance of three individuals: the subject, a person to drive CW-6 fNIRS software, and a person to manipulate the PPG. The person manipulating the PPG has PowerPoint cue that runs the entire 8 blocks signaling when to press the set or reset button. The pressure pump is connected to the pressure accumulator via pneumatic air tubing and the vacuum source is connected to the vacuum accumulator. Next the pressure pump is turned on to create a pressure reservoir in the pressure accumulator the vacuum pump is also turned on. As pressure is filled in to the accumulator, the pressure gauge on the PPG reveals the real time pressure in the pressure accumulator. Once optimal pressure to operate the pressure/voltage transducer is reached, the vacuum pump is turned off. Next the subject is seated with arm resting on the laboratory bench top so that the mechanical stimulation apparatus that propels the aluminum target could be properly mounted. The apparatus is mounted on the table top with respect to the point of interest on the arm. Next the CW-6 with the respective channels are secured to the head of the subject with Velcro

and a bandage is further used to secure the channels to the subject's head. Once the CW-6 is calibrated, the subject is asked to remain still and meditate on peace thoughts. The person controlling the CW-6 software gives the cue to initiate timing of the 8 blocks with each block being 40 seconds in duration. The start time of the CW-6 software and PPG PowerPoint are synced so that the hemodynamic response can be directly corrected to the time of stimulation and non-stimulation for the duration of the protocol. Once the time begins, the person operating the PPG monitors the PowerPoint to know when to press the set or reset button. There is a 40-second pre-stimulation period; there is a 4-second period that consist of two sets and resets as described in Figure 2.6. This is followed by 36 seconds of rest. Within the 4 seconds, the inter-stimulus time is 1 second. One block is 4 seconds of stimulation followed by 36 seconds of rest. This is repeated 7 more times.

3.2 Calibration Curve

The calibration curve is essential for the correlation between the voltage at which the subject rated the pain and intensity of the pain. Figure 3.3 is the calibration curve of the Marsh Bellofram pressure-voltage transducer that was used for my study. In order to determine the calibration curve, the pressure pump was connected to the PPG and power was supplied. Once the pressure spec for the transducer was reached (via monitoring the pressure accumulator gauge), recording of the voltage and corresponding pressure/voltage transducer output pressure began. Voltage was modulated via the transducer power supply (see Figure 2.2 and 2.3). One method was done by setting the output pressure of the transducer to 4psi via the transducer power supply and incrementing the output pressure by 2psi by manually adjusting the voltage on the power supply. As the pressure was increased by 2psi it's corresponding voltage was recorded. Another method was done by starting at 0.6 V and incrementing by 0.2 V and recording the corresponding pressure. Both were done to assure functionality and consistency of the PPG.

Figure 3.3 demonstrates a linear relationship between the pressure used to propel the target to the skin and the corresponding voltage. As voltage increases, the pressure simultaneously increases also. The increase in pressure moves the target of a defined mass to have a bigger impact on the skin.

This aspect of the Pressure Pain Generator provides the information necessary to correlate the pressure with the subject's pain. It also provides a standard at which pain can be reproduced at the same mechanical intensity, as well as with the same degree of pain stimulus used for the protocol. The correlation coefficient ($R^2 = 0.9998$) between the pressure and voltage demonstrates how accurate the output pressure can be predicted based on the input voltage.

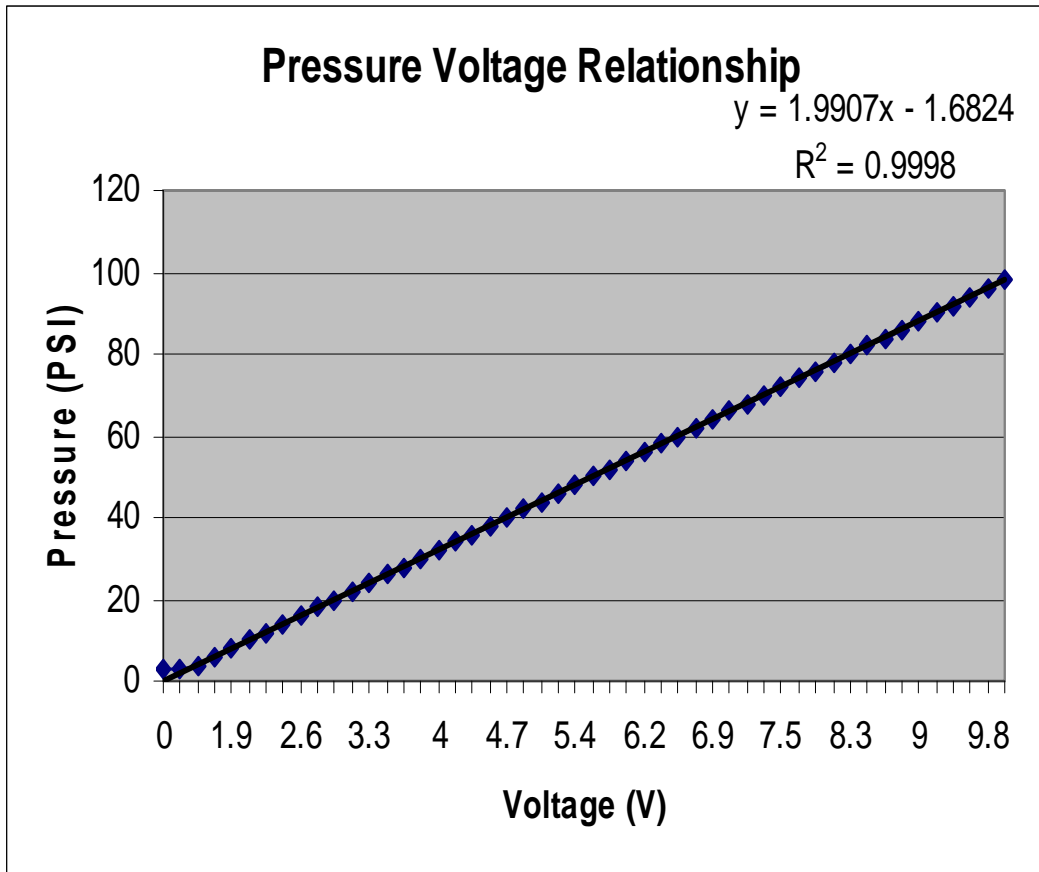


Figure 3.3 Pressure-Voltage relationship derived from the E/P Transducer

3.3 Implementation of the Pressure Pain Generator and Use of fNIRS for Human Study

The following results support the feasibility of using the Pressure Pain Generator to create controlled pain in conjunction with fNIRS measurement to study the associated hemodynamic responses in the prefrontal cortical regions of the human brain.

3.3.1 *Subject's Pain Threshold and Corresponding Voltages*

The subject's pain threshold rating was determined by finding the subject's perception of the pain. Table 2.1 shows the results of the subject's pain level up to the maximum tolerant intensity of pain. Once the subject's peak tolerance was determined, the mechanical pain stimulation was done at 30% and 60% of the peak pain. Table 2.1 highlights 30% and 60% of the subject's threshold, which corresponds to pain level 3 and 6, respectively. It is interesting to note that as the voltage increases, the subject's pain level remains stagnant within a certain range before the subject's perception of pain changed. Once the subject started feel increment of pain, the pain rating increased each time. The subject's pain intensity levels of 3 and 6 were performed at 1.2 V and 2.0 V, respectively, using the block design.

Table 3.1 Subject pain rating chart and corresponding pain scale

Voltage (v)	Pain Rating
0.6	3
0.8	3
1.0	3
1.2	3
1.4	3
1.6	4
1.8	5
2.0	6
2.2	7
2.4	8
2.6	9
2.8	10

3.3.2 Temporal Changes in Oxygenated Hemoglobin Concentration due to Pain Stimulation

A two dimensional map can be used to show changes in oxygenated hemoglobin concentration (dHbO) that varied across different regions. On the other hand, changes in concentration of oxygenated hemoglobin and deoxygenated hemoglobin over time at a specific location can be shown by a temporal profile as a graphical representation. Figure 3.4 provides the physical representation of each detector and respective source. Each source can pair with up to six detectors. The measurements from all the channels provide us with the data necessary to generate temporal plots for each source-detector pair that reflect local changes in oxygenated hemoglobin concentration.

To determine significant changes induced by pain, a comparison between the stimulation results and the baseline results were assessed. Student t-test was performed to determine if there was any significant difference ($p < 0.05$) between the stimulation and baseline data. The comparison was done on a channel by channel basis. Figure 3.4 again displays a graphical representation of sources (red circles) and detectors (blue circles) and all possible channels (i.e., source-detector pairs). Note that source 1 was placed on the right lateral frontal side, while source 3 was on the left lateral frontal side.

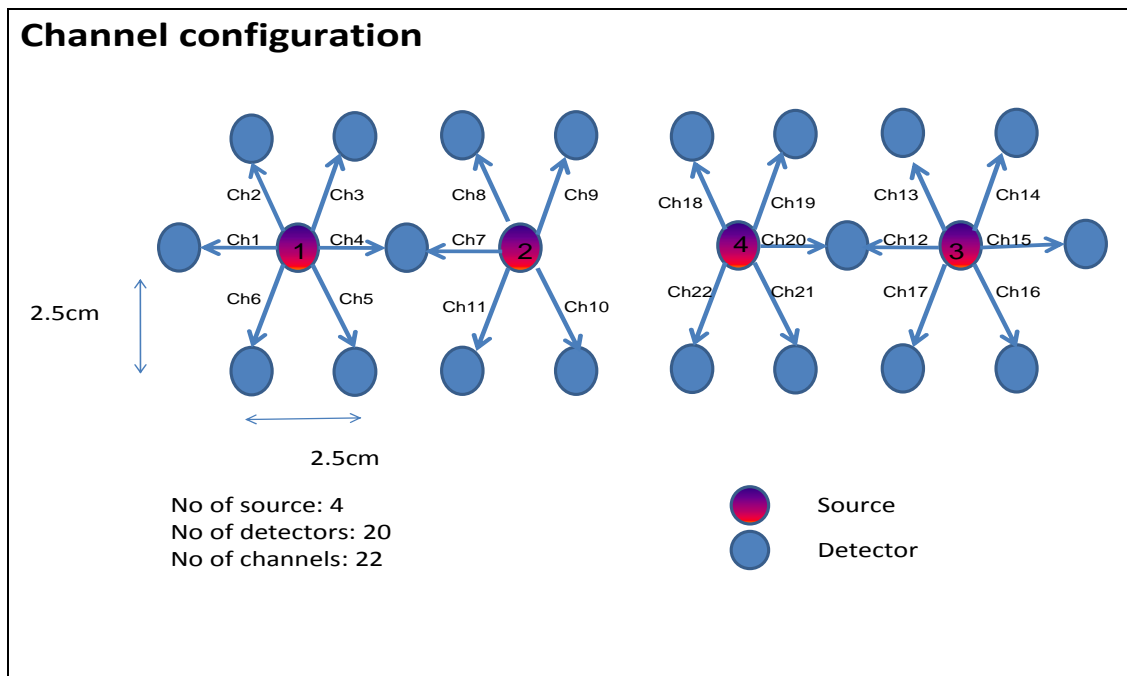


Figure 3.4 Configuration of source-detector pairs (channels)

Figure 3.5 shows an example of temporal plots of changes in HbO (ΔHbO), with Source 2 being the light source location and Channels 7 to 11 recording the signals, as marked by Figure 3.5(a), which is the graphical representation of figure 3.4. The respective colors on Fig. 3.5(a) are specific to each channel and are translated onto Fig. 3.5(b). The red bar shows the time segment selected to average the temporal signals to reconstruct the image in Fig. 3.5(c). Figure 3.5(b) shows the respective ΔHbO

traces from the channels identified. Figure 3.5(c) displays three reconstructed images of HbO, HbR, and HbT ($=\text{HbO}+\text{HbR}$), with the signals averaged over the selected time window (5-15 sec), as marked in Fig. 3.5(b). The temporal profiles of HbO in Figure 3.5(b) display large deactivation in oxygenated hemoglobin concentration. It can be noted that channel 9 displays the greatest degree of change. This channel appears to deviate from the rest of the other channels due to its great negative change in HbO, as compared to the other channels. The set of data were taken from the subject under pressure stimulation at a pain level of 3.

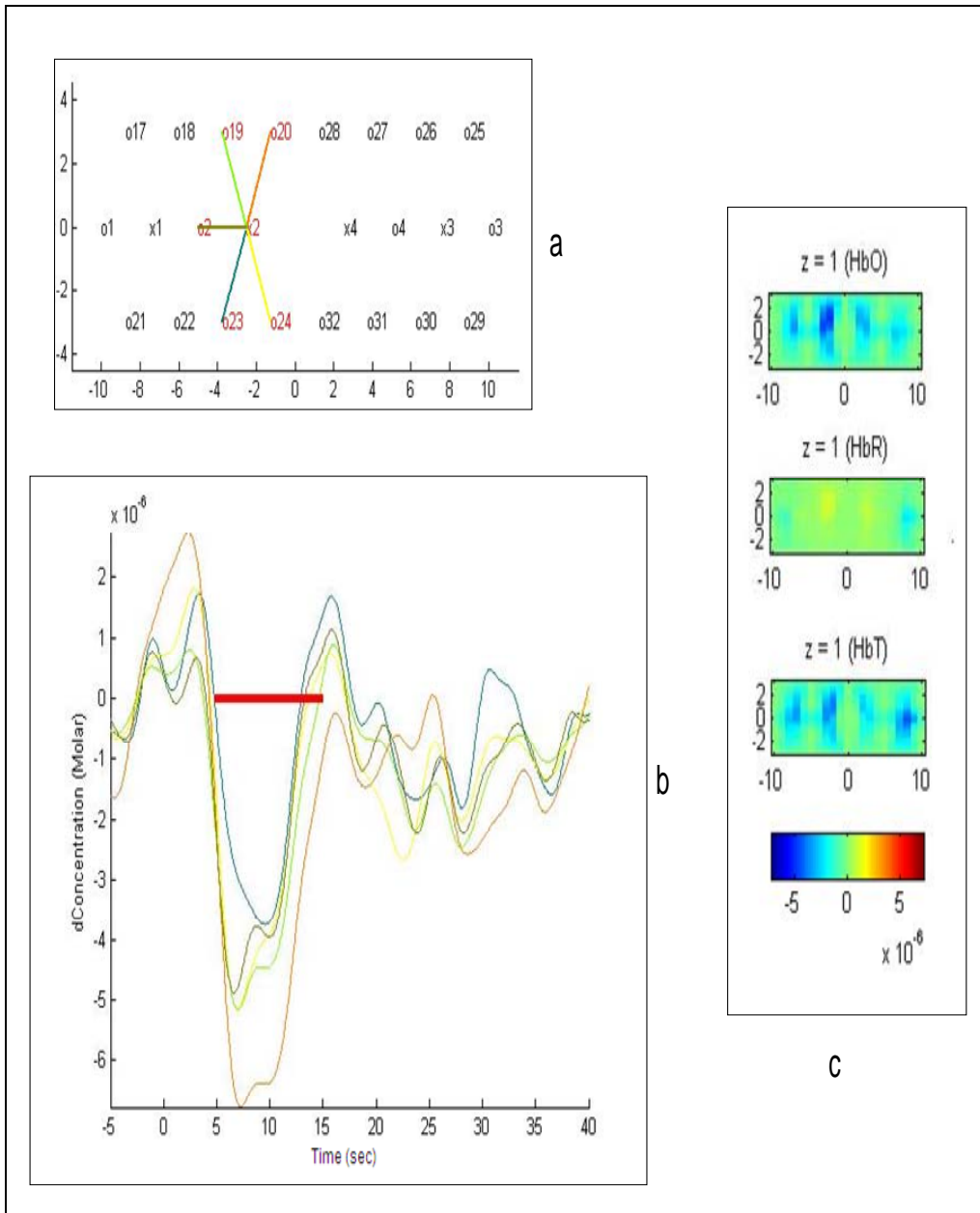


Figure 3.5 (a) Selected channels with Source 2 being the light source configuration; (b) corresponding temporal Δ HbO plots from the selected channels; (c) corresponding reconstructed HbO, HbR, and HbT images from a subject with pressure stimulation at a pain level of 3.

Figure 3.5 shows the effectiveness of the Pressure Pain Generator (PPG) to stimulate pain that could be recordable by fNIRS. Since Figure 3.5 displayed data at pain level 3 only from Source 2, the remainder of the plots for Sources 1, 3, and 4 at pain level 3 and the plots with Source 1 to 4 at pain level

6 are given in Appendix A, for further reference. Overall, all the temporal profiles from different sources and detectors, namely at different channels, demonstrated consistent changes in HbO in response to pressure-induced pain over time. Interestingly, before the pain stimulus was applied (-5 to 0 sec), there was a slight elevation in the delta concentration, which continued into the stimulus time (0 to 5 sec). However, there was a large decrease in the concentration of HbO post-stimulus (5 to 15 sec). These decreases in HbO was stopped and promptly returned toward the baseline around 15 seconds. Similar effects were also seen in pain level 6 data (see Appendix A). Such visual observation on these temporal profiles shows supporting evident for the effectiveness of the Pressure Pain Generator.

3.3.3 *Graphical Comparison of Change in Oxygenated Hemoglobin Concentration Over Time*

To assess the significance of the temporally varying change in HbO concentration, statistical analysis using Student paired t-test was done. As it is expected, there was no difference between pre-stimulus data (-5 to 0 sec) of baseline results and pain stimulation results (0-5 sec). However, during stimulation (0 to 5 sec) and post-stimulation periods (5 to 15 sec, 15 to 30 sec, and 30 to 40 sec), signals from most of the channels were significantly different ($p < 0.05$). Channels that reported to have non-significant changes might have been a consequence of source-detector pair placement, hair interference, or some other physiological phenomenon. Figure 3.6 is a comparison plot of the mean ΔHbO values and standard deviation from each channel taken during the pre-stimulation (0-5 sec) and 5-15 seconds time span with pain level 3 (see Figure 3.5(b) for the corresponding temporal changes in HbO at different channels). Recall that Fig. 3.5(b) showed the excessive change in HbO temporal profile from channel 9; this is also evident in Figure 3.6. Notice that channel 9 shows the greatest deactivation in HbO.

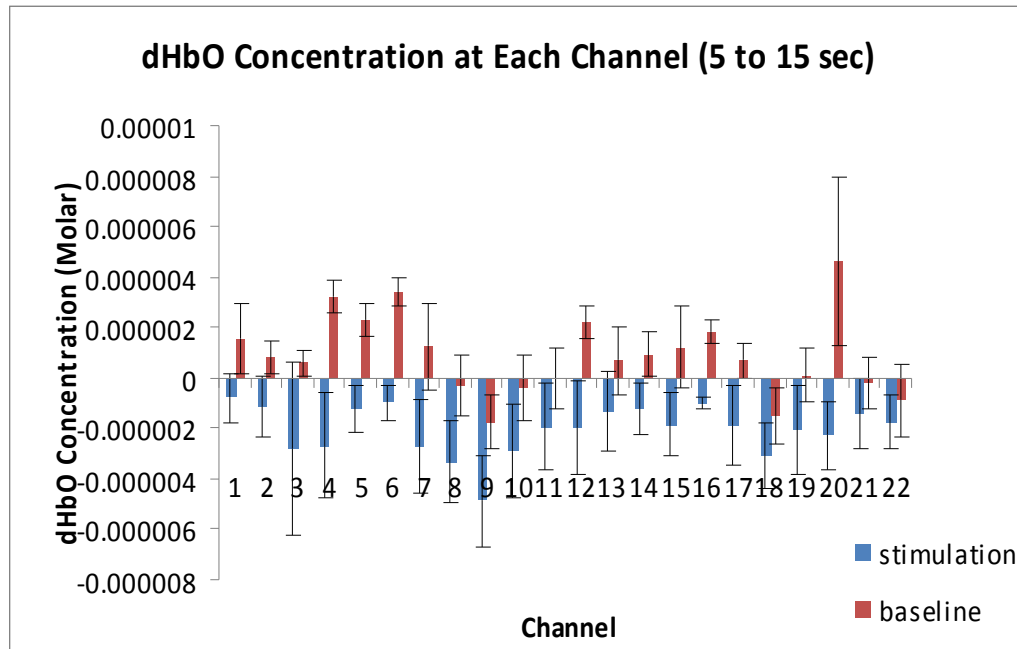


Figure 3.6 Averaged changes in HbO at each channel over the 5-sec baseline (blue bars) and 5-15 seconds post-stimulation (red bars), with pressure stimulation of pain level 3; Error bars: the standard deviation.

Averaged changes in HbO at each channel between the 5-sec baseline (blue bars) and the post-stimulation (5-15 sec), as represented in Figure 3.6, are statistically different. This set of data supports the application of the Pain Pressure Generator which can create controlled pain, based on the fact that post stimulation (5 to 15 sec) results showed great changes in HbO amplitudes. Indeed, the changes indicate strong deactivation of HbO over all 22 channels, which is different from common positive responses to many cognitive functions. Also, in comparing the HbO profiles between the pre-stimulation (5 to 0 sec) and post-stimulation (5 to 15 sec, 15 to 30 sec, and 30 to 40 sec) at both pain levels, there were significantly more channels showing a negative change in HbO during the post-stimulation. During pre-stimulation, most of the channels show a positive trend in HbO, similar to the baseline shown in Fig. 3.5(b). These time segments were selected to assess the hemodynamic responses to pain before, during, and after the pressured-induced pain stimulation. Additionally, graphical plots to compare averaged changes in HbO between the stimulation and baseline period across all 22 channels are

represented in Appendix B, for further information.

An odd occurrence was observed at channel 20 during baseline data analysis. Channel 20 expressed extreme change in HbO concentration. Since baseline data was not collected on the same day as stimulation data, there might have been some interference from hair, failure on the respective detector to function as expected, or some physical difference in the positioning of the source-detector pair. This was not evident during stimulation.

The spatial profiles (e.g., those in Figure 3.5) at the selected temporal window were assessed. This was the time segment after pain stimulation was stopped. This time interval, which displayed the most channels to show significant differences in HbO between the baseline and stimulation (Figure 3.6), was used to also assess the effect of the pain generator. This period of interest (5-15) is best represented hemodynamic response after pain stimulation ceased for both pain level 3 and 6 with the most number of significant channels. Figures A.1 to A.8 in Appendix A can support this statement.

3.3.4 Spatial Profile of Change in Oxygenated Hemoglobin Concentration Over Time

For the purpose of demonstrating feasibility of the Pressure Pain Generator, channel 9 was selected for discussion purposes. Channel 9 is one of the channels that successfully demonstrated a statistically significant change in the hemodynamic response after mechanical stimulation was applied. Figure 3.7 is the spatial plot depicting the hemodynamic response for pain levels 3 and 6. According to the image reconstruction, pain levels 3 and 6 displayed similar responses before, during, and after stimulation. Their images are placed side by side in Figure 3.7. The most alluring segment was the 5-15 seconds plot. The 5 to 15 seconds time segment has several channels expressing large deactivation (decline in HbO concentration). Based on the hemodynamic response scale, activation is represented towards the red while deactivation is towards the blue. Examining the area near channel 9 in Figure 3.7, it is clear to see activation (positive change) in HbO concentration during stimulation (0-5 sec), followed by a strong deactivation immediately after stimulation (5-15 sec). Figure 3.4 can be used to locate channel 9.

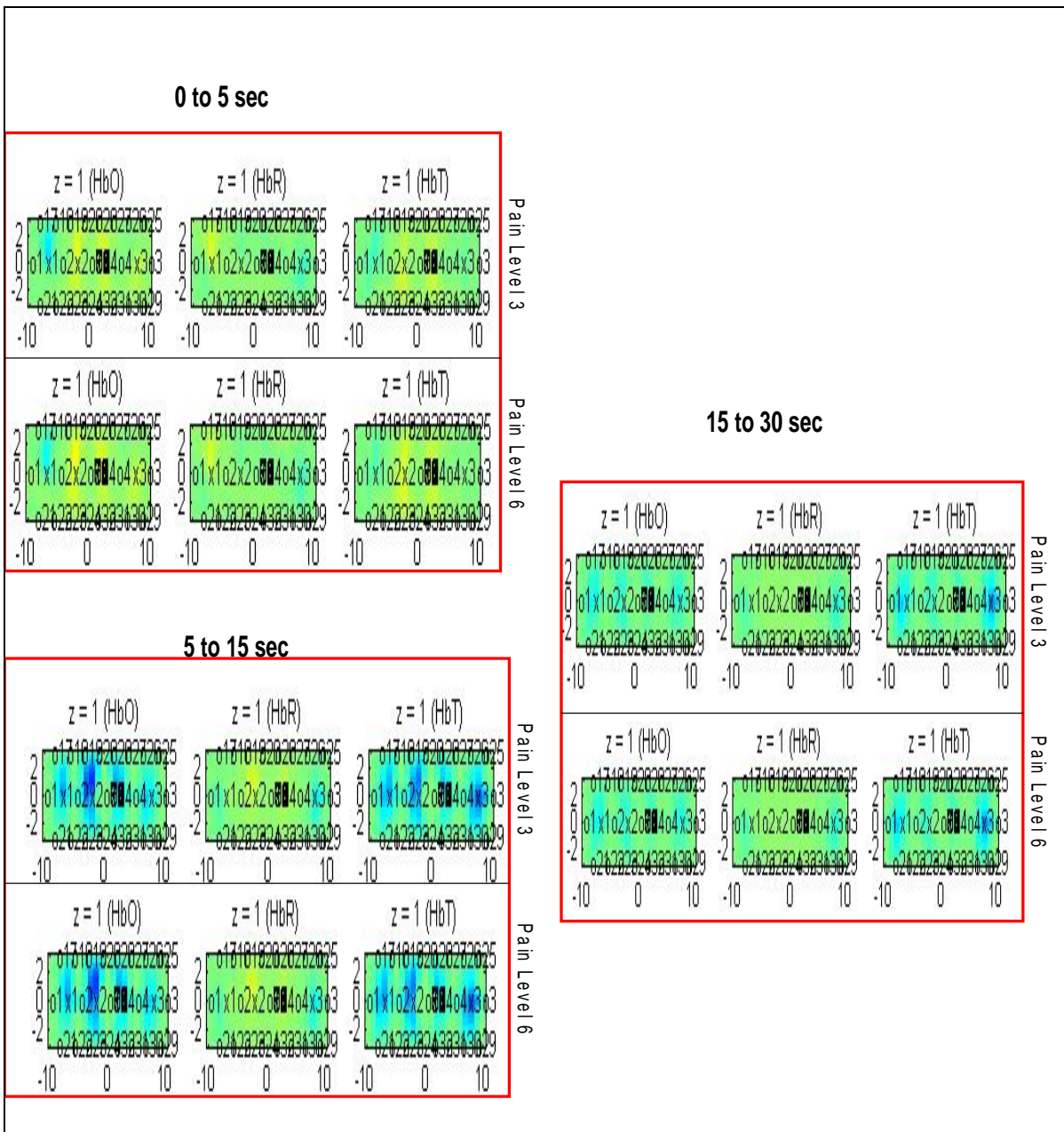


Figure 3.7 Time-dependent spatial profiles of HbO at pain levels 3 and level 6 over time.

CHAPTER 4

DISCUSSION AND CONCLUSION

4.1 Discussion

This research was a feasibility study to implement, realize, and evaluate a pressure-controlled pain generator (PPG) as well as to demonstrate its success in creating controlled mechanical pain. In addition, while inducing controlled pain, this pressure-induced pain generator can be also used with an fNIRS instrument to correlate the pain evaluation with hemodynamic responses measured in the prefrontal cortex. This feasibility study contained a single subject that was tested to investigate functional activation or deactivation within the prefrontal cortex using fNIRS. The results indicate that pain was created with a good control by this PPG and was measurable. The time-dependent hemodynamic images in response to the pain stimuli indicated that there are significant changes or decreases in the concentration of oxygenated hemoglobin in the post-stimulation period. The figures located in Appendix A provide details on the temporal pattern and the spatial characterization at the time segment when the greatest negative change was detected and statistically significant (5 to 15 sec). The results clearly represented deactivation immediately post-stimulation. Furthermore, the statistical plots of the change in HbO concentration due to pressure stimulation at each channel, as assessed in comparison to those taken during baseline, showed strong evidence of feasibility of the Pressure Pain Generator.

However, there was non-trivial variability in the hemodynamic responses seen in various channels. It is important to note that placement of the fNIRS sources and detectors affect the optical signals critically. There were some channels that reported weaker signals and some stronger signals (see Appendix B). This was evident in both pain level 3 and level 6. Also, channel 20 reported some skeptical results during the baseline measurement. Since the baseline data collection was not repeated, it could be determined if it might have been an error in the probe setup or a physical defect of the channel.

The temporal assessment provided a reference point from which the hemodynamic responses to mechanical pain stimulation can be studied. Lopez-Sola et al. [10] provided evidence of the presence of anticipatory activation in the promoter-prefrontal region which was not addressed in my study. Lopez-Sola et al. used fMRI, while this study utilized fNIRS on the prefrontal cortex. Lopez-Sola et al. [10] provided evidence supporting the role the lateral frontal cortex played in pain processing. Two to four seconds after the anticipatory audible cue was given, activation in the premotor-prefrontal cortex was increased and peak 4 to 6 seconds after the initial tone. Their results showed that hemodynamic activation was present during the stimulation; however, once stimulus was removed, the activation gradually declined. In this feasibility study, similar results were seen. In assessing the time-dependent files of the hemodynamic response, it was seen that the temporal and spatial dynamic changes returned toward their baselines, once the pain stimulus was removed. In comparing pre, during, and post stimulation in this study, no evidence of anticipation was expressed, but some level of activation was present during the early phase of stimulation; . With respect to the location of activation/deactivation in prefrontal cortex, both fMRI and fNIRS showed a positive correlation with mechanical pain during the instance of pain stimulus. Lui et al. [21] also reported similar finding with fMRI. In the medial prefrontal cortex, there was significant decrease in signal after tactile and painful stimulus.

In understanding functional neuronal/hemodynamic signals with respect to the perception of pain, one fMRI study revealed that a decrease in signal activation correlated to a decrease in pain perception [24]. This was consistent with this study. During mechanical stimulus application, the subject reported pain at the instance when pain was applied, but as stimulus was removed, the pain intensity felt was significantly reduced. The reduction in reported pain perception during post-stimulus is supported in the strong deactivation present on the temporal profile. In addition, analyzing the fNIRS hemodynamic temporal profiles provided additional evidence. However, decrease in activation during post-stimulus has been associated with expecting the painful stimulus or having memory of the stimulus. According to the study by Wiech et al. [25], which supports the conclusion by Lopez-Sola et al. [10], expectation increases activation signal during stimulation. If a cue signal is present, prior to stimulation, the activation signal

elevates, thereby enhancing the perception of pain. Another biasing of pain perception was based on the fact that if subject was cued to expect low pain, then there was less activation was seen when compared to be cued to expect high pain [25]. Neuronal processing of pain perception during stimulation is pre-determined by knowledge of the stimuli, whether through experience or cues. In the case of this feasibility study, it is possible that the experiential knowledge of the pain intensity might have affected the subject's neuronal/hemodynamic response, according to Wiech et al. [25]. Such experiential knowledge of the pain level may result in a decrease in activation during post-stimulus and also a decrease in the pain perception according to Bantick et al [24].

Pain is modulated in the prefrontal cortex because it receives sensory input from the limbic system and shares a relationship with the motor cortex, such that based on the intensity of pain perceived, the prefrontal cortex communicates to other tissues to respond accordingly [25]. There are many factors that can affect the signals measured by fNIRS during mechanical stimulus. If adaptive filters can be used, it would help to remove systemic and physiological interferences so that the signals measured will be cleaner or less contaminated by other interferences. Muscle twitch could also add confounding factors to the cognitive processes in the prefrontal cortex. EMG measurements could be used to identify and exclude muscle movement

4.2 Conclusion

In summary, the pressure-controlled pain generator was realized and functioned as expected. The Pressure Pain Generator showed reproducibility in generating controlled levels of mechanical pain through the pressure/voltage relationship via the transducer. Pain levels could be quantified using pain scale and rating accordingly. The method to stimulate mechanical pain is a feasible tool in conjunction with functional near infrared spectroscopy to study brain response to pain. It shows promise in assessing hemodynamic response of pain in the prefrontal cortex and correlating it to the different degrees of mechanically induced pain.

4.3 Future Work

Since this study utilized only one subject to do the preliminary assessment of the Pressure Pain Generator, more subjects are needed to carry the study. Also, subjects recruited in the future should not be informed of the protocol so that the expectation bias can be eliminated. Secondly, the stimulus protocol should incorporate instance where the subject is deceived to believe that painful stimulus will be applied but it is not really performed, and also instance where the subject is just surprised. By also varying the pain level, the subject does not get familiar with the degree of pain, thereby not biasing the results. Possibly the time period for stimulation should be extended to see if adaption takes place.

APPENDIX A

RAW DATA OF CHANNELS WITH
CORRESPONDING TEMPORAL
AND SPATIAL PROFILES

The following figures represent the channel configuration, temporal profile and spatial profile at the time segment showing the greatest change in oxygenated hemoglobin concentration post-stimulation (5 to 15 sec). This is raw data in HomER. The criteria used to determine which channels are to use to generate the temporal profile was based on channels exhibiting significance at the standard of $p < 0.001$.

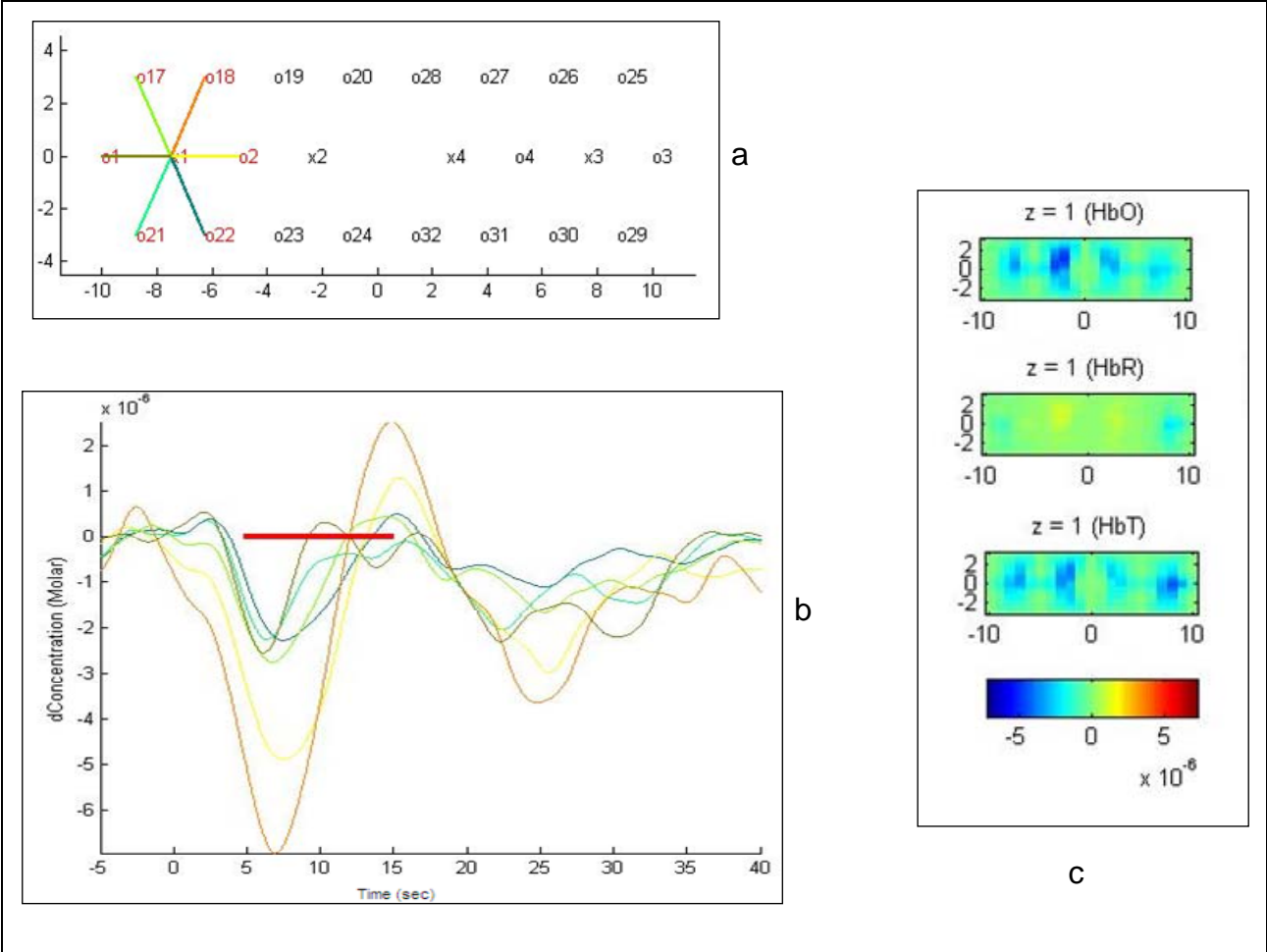


Figure A.1 Source 1 - Channel configuration (a), corresponding temporal (b) and spatial (c) plots of subject with a pain level of 3.

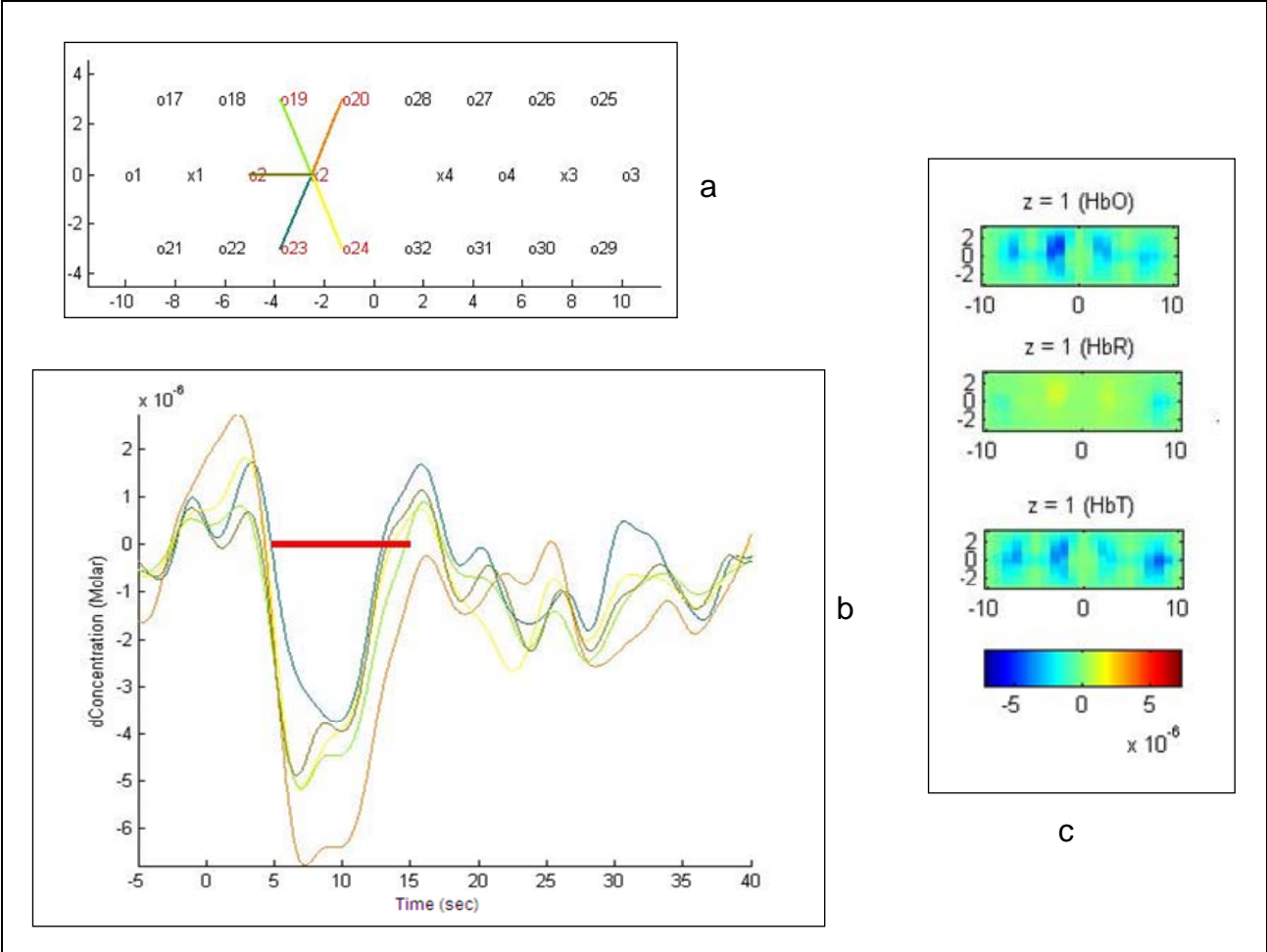


Figure A.2 Source 2 - Channel configuration (a), corresponding temporal (b) and spatial (c) plots of subject with a pain level of 3.

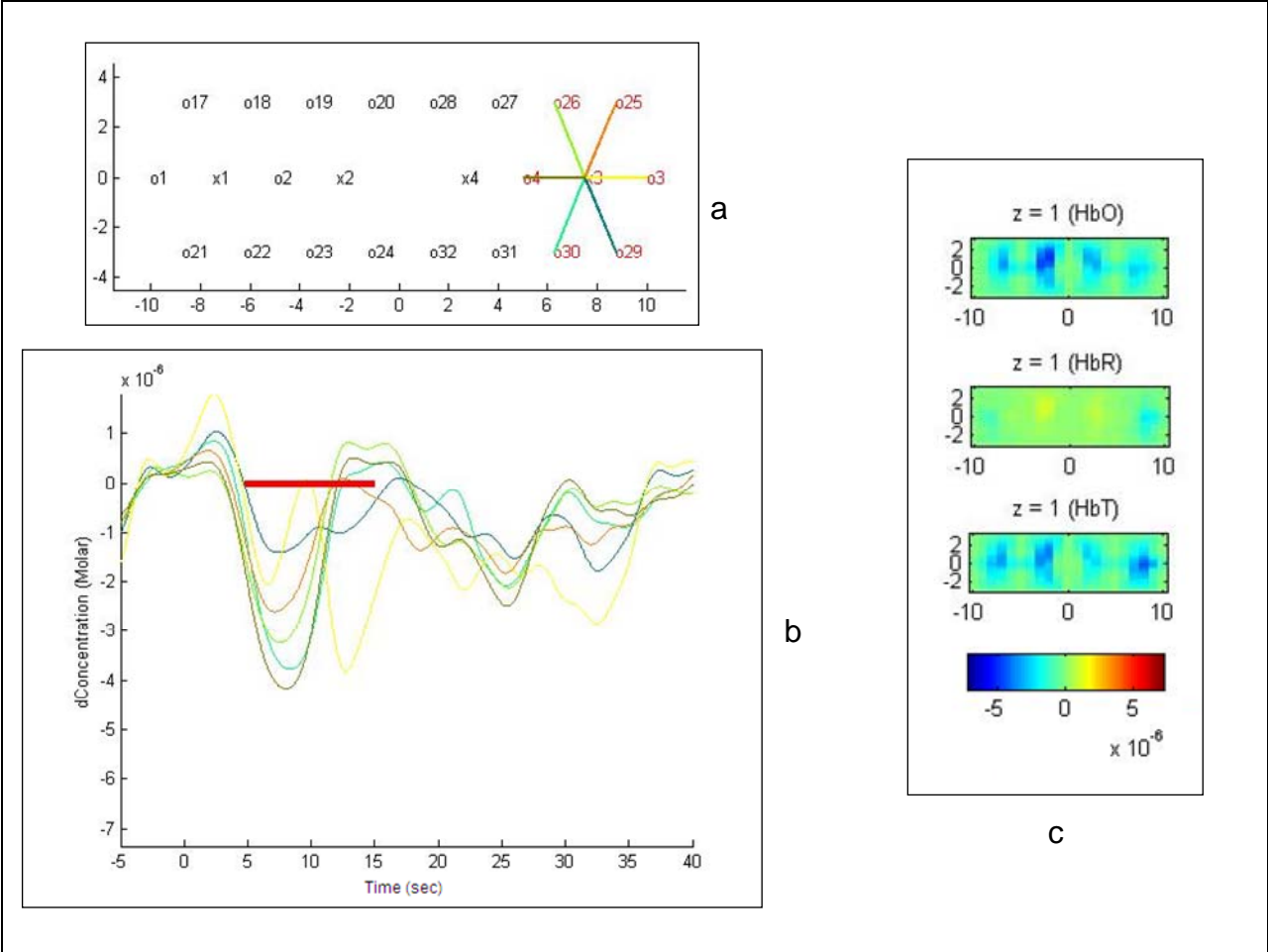


Figure A.3 Source 3 - Channel configuration (a), corresponding temporal (b) and spatial (c) plots of subject with a pain level of 3.

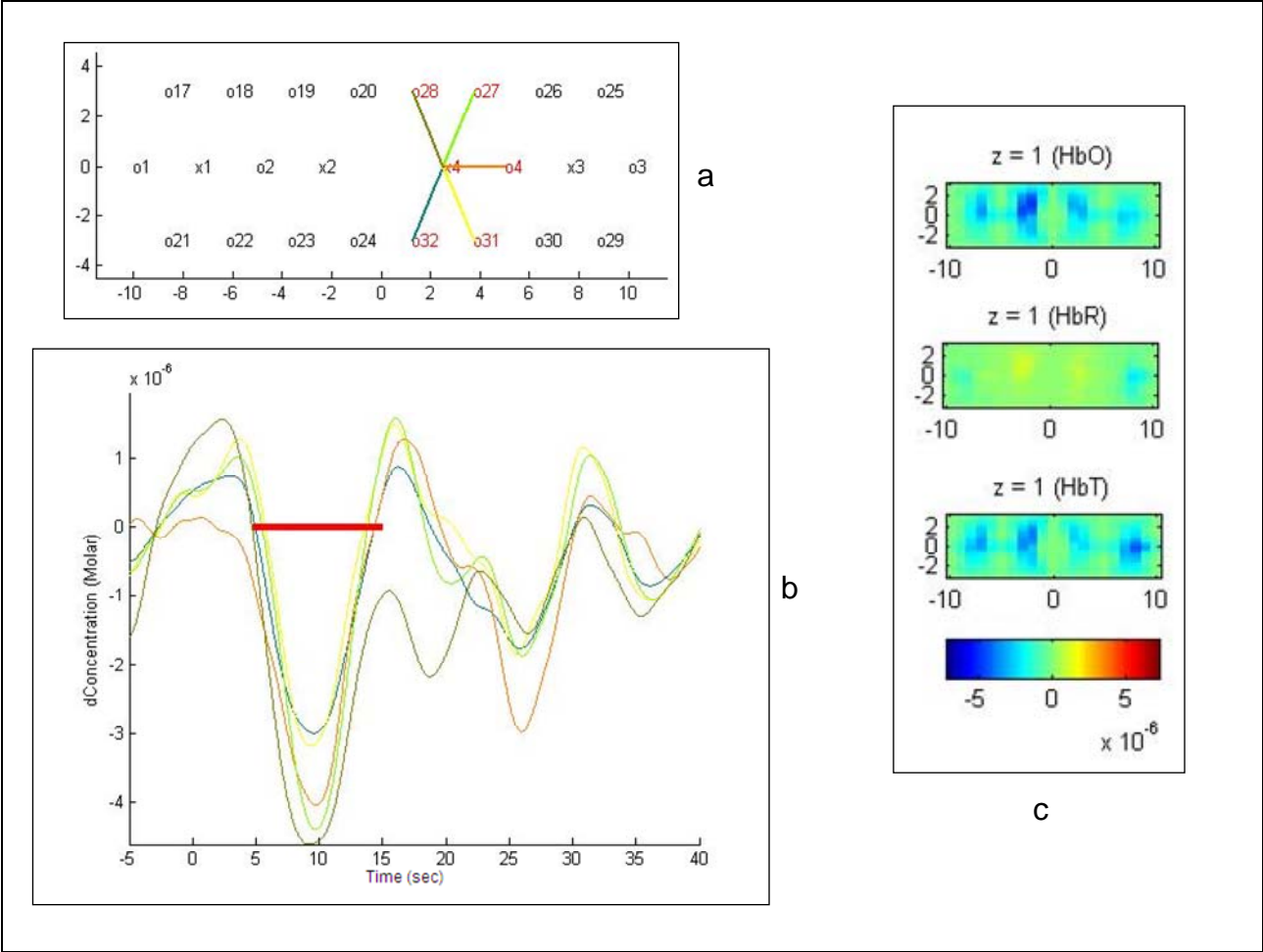


Figure A.4 Source 4 - Channel configuration (a), corresponding temporal (b) and spatial (c) plots of subject with a pain level of 3.

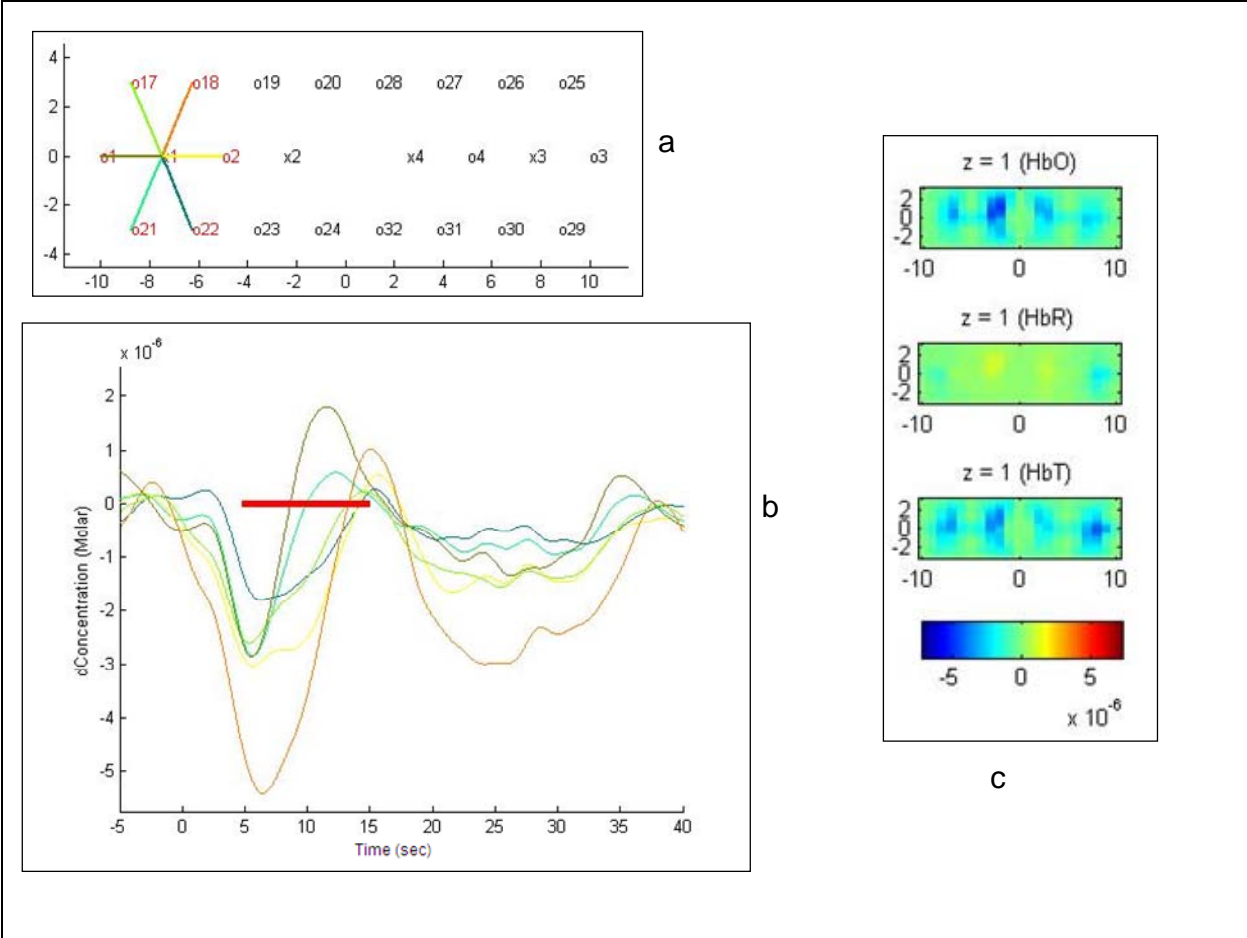


Figure A.5 Source 1 - Channel configuration (a), corresponding temporal (b) and spatial (c) plots of subject with a pain level of 6.

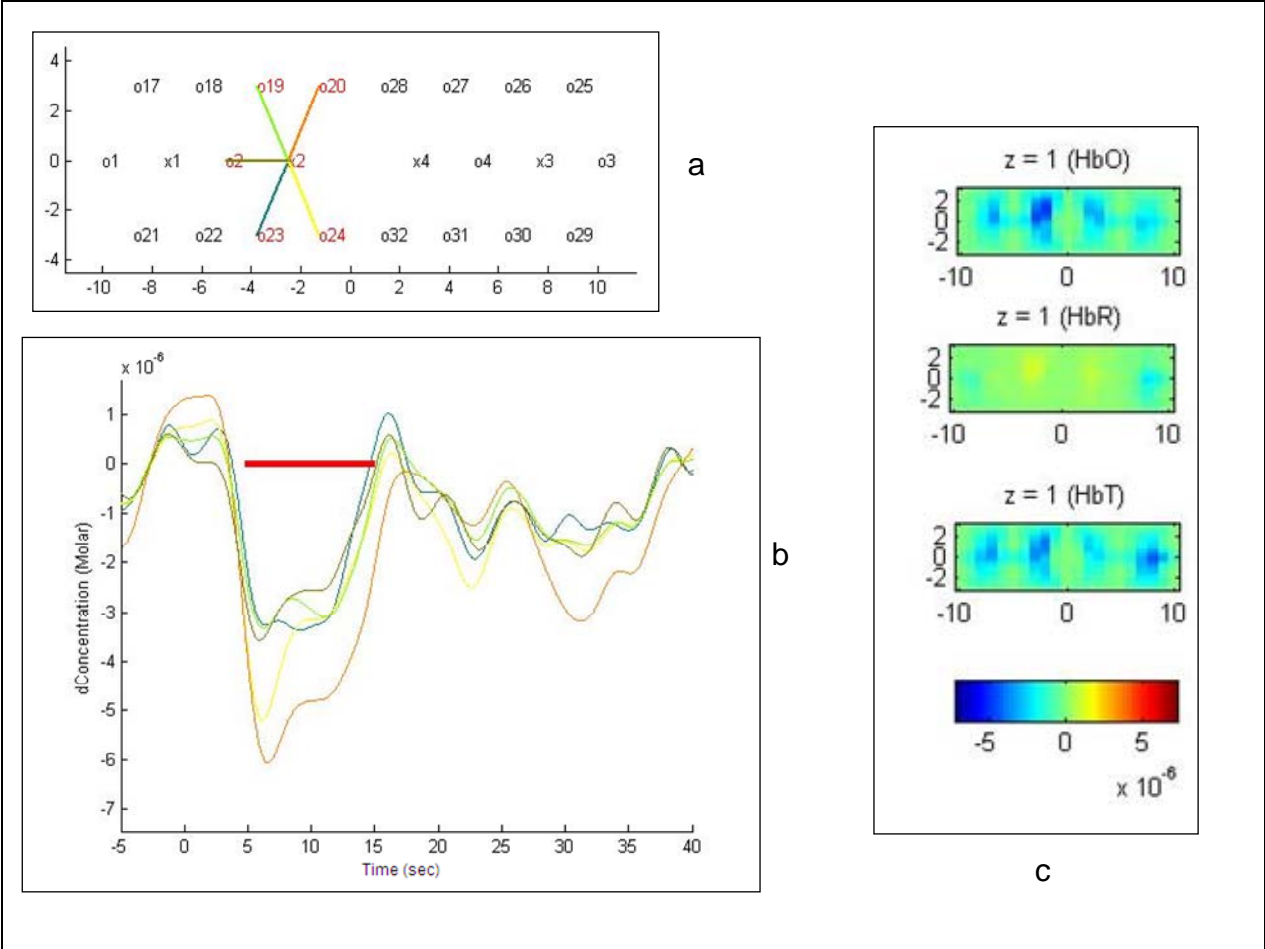


Figure A.6 Source 2 - Channel configuration (a), corresponding temporal (b) and spatial (c) plots of subject with a pain level of 6.

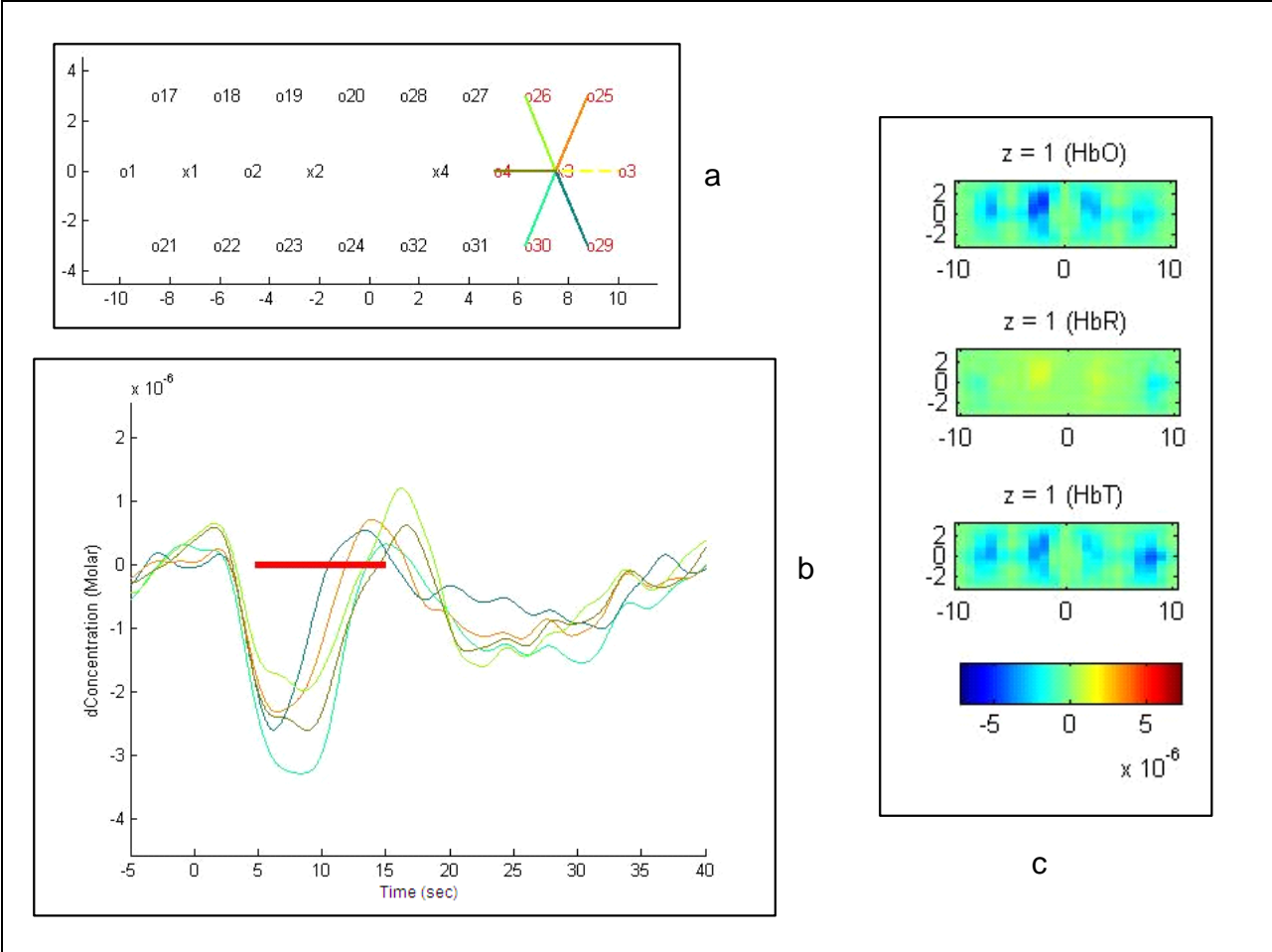


Figure A.7 Source 3 - Channel configuration (a), corresponding temporal (b) and spatial (c) plots of subject with a pain level of 6.

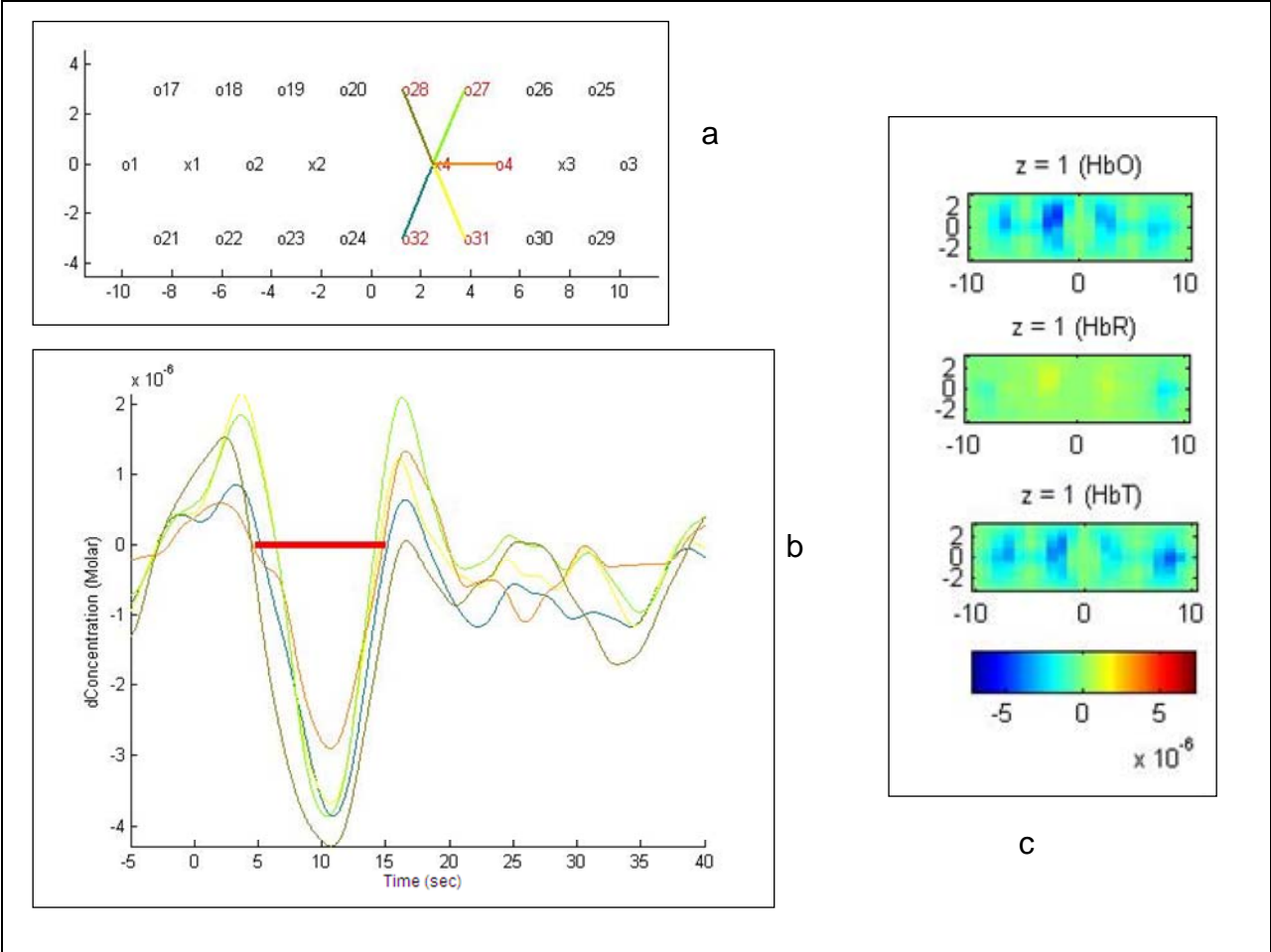


Figure A.8 Source 4 - Channel configuration (a), corresponding temporal (b) and spatial (c) plots of subject with a pain level of 6.

APPENDIX B

RAW DATA COMPAREING MEAN CHANGE
OF OXYGENATED HEMOGLOBIN
AT EACH CHANNEL

Appendix B is the graphical plots of the raw data comparing the means of changes in oxygenated hemoglobin between the stimulation and baseline period across all 22 channels. It displays the data at the different time segments, pre-stimulation, during stimulation, and post stimulation with the standard deviation as the error bar. Both pain level 3 and 6 are represented. The interesting item to note is the suspicious peaks of channel 7 and channel 20 at baseline. Since baseline data was collected on a different day, it is possible that the two channels might not be functioning as expected, or their placement on the forehead might be the issue.

PAIN LEVEL 3 MEAN PLOTS

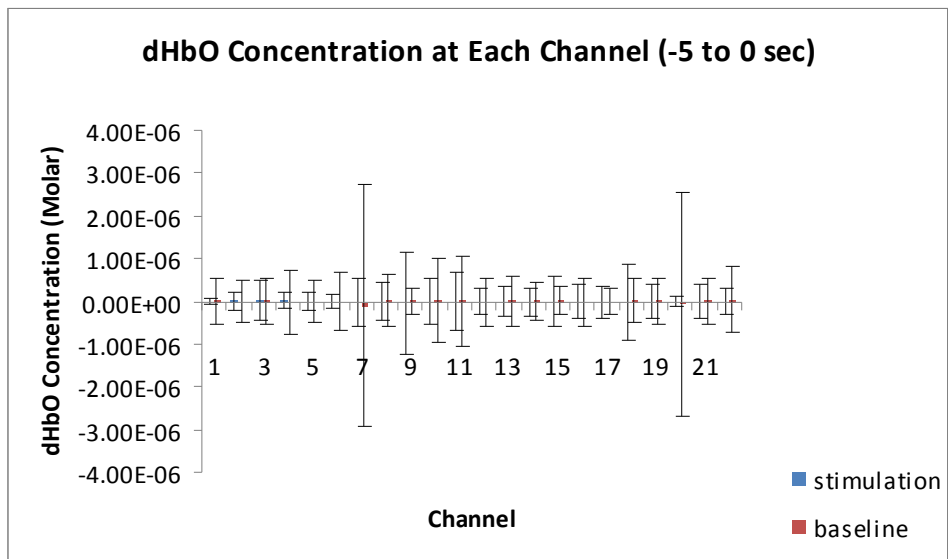


Figure B.1 Mean of the change in oxygenated hemoglobin at each channel over 0 to 5 seconds.

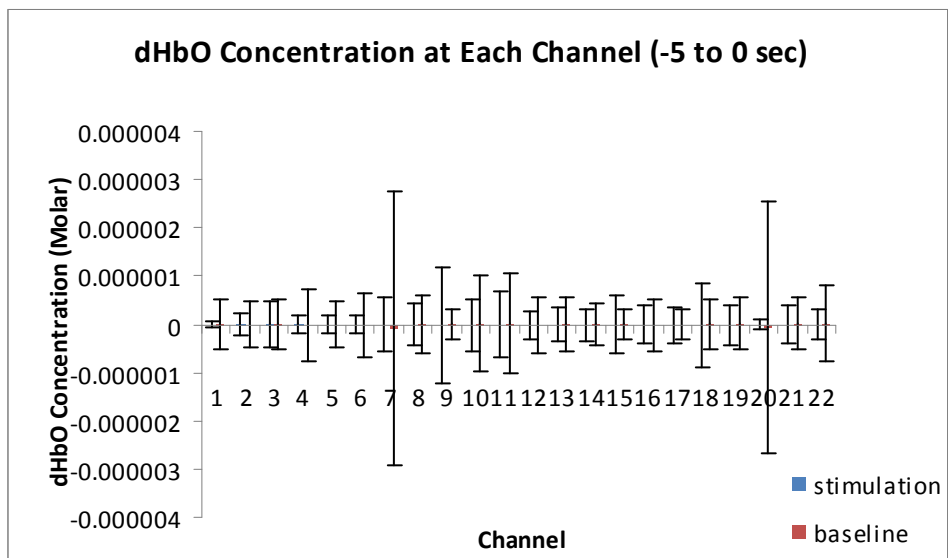


Figure B.2 Mean of the change in oxygenated hemoglobin at each channel over -5 to 0 seconds.

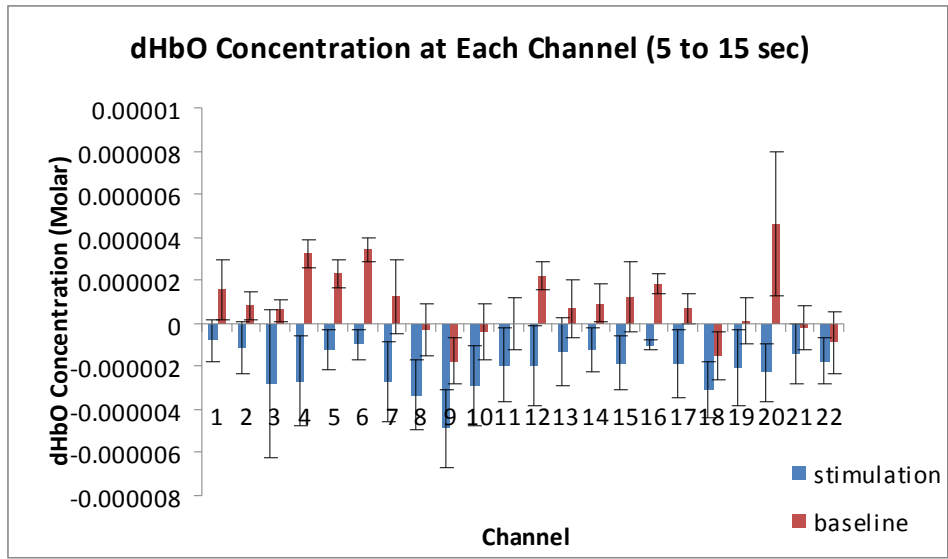


Figure B.3 Mean of the change in deoxygenated hemoglobin at each channel over 5 to 15 seconds.

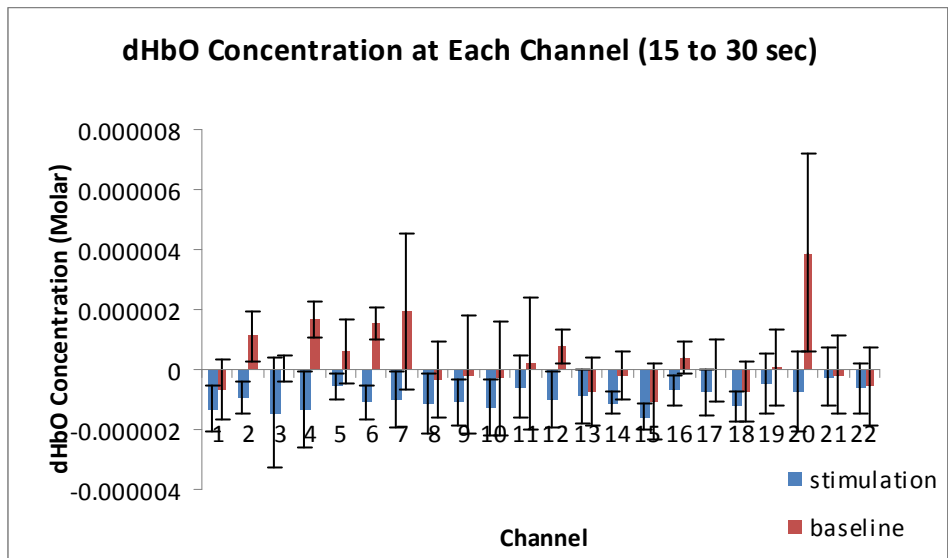


Figure B.4 Mean of the change in deoxygenated hemoglobin at each channel over 15 to 30 seconds.

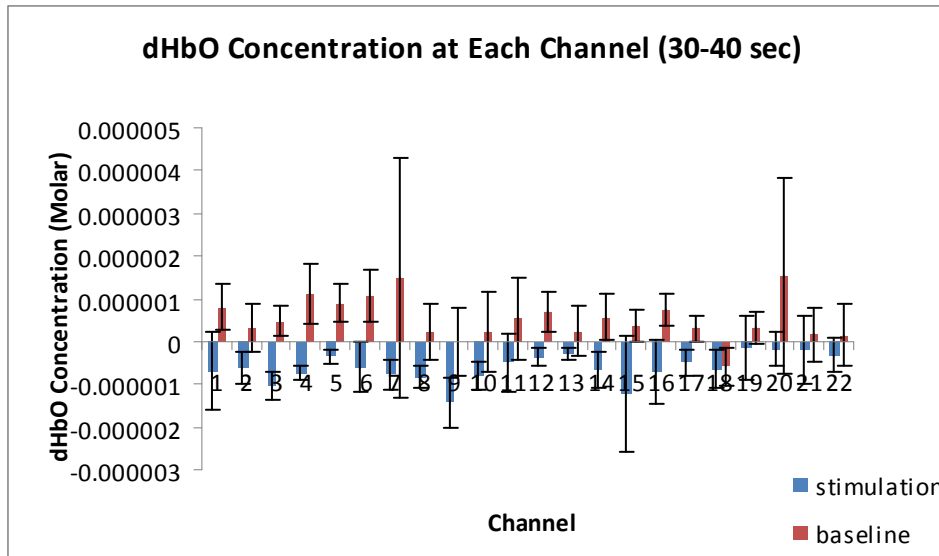


Figure B.5 Mean of the change in deoxygenated hemoglobin at each channel over 30 to 40 seconds.

PAIN LEVEL 6 MEAN PLOTS

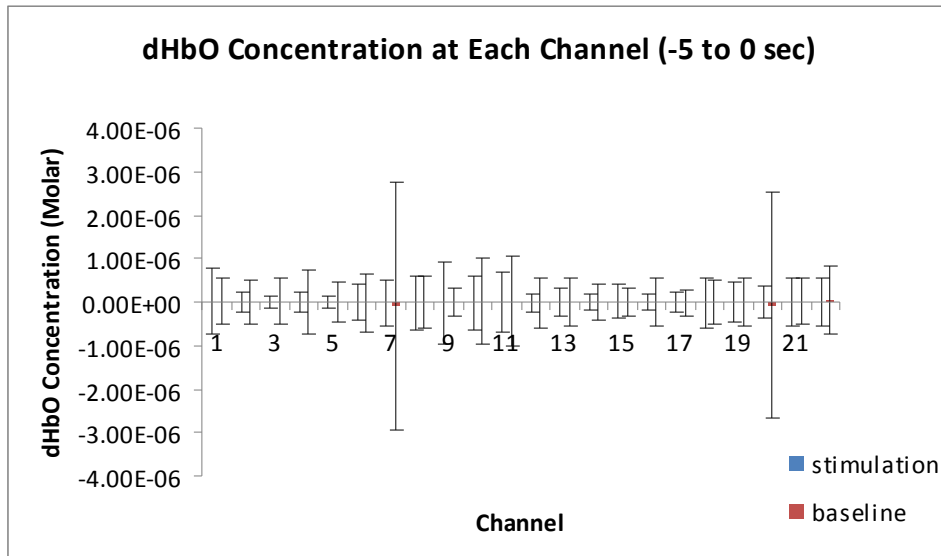


Figure B.6 Mean of the change in deoxygenated hemoglobin at each channel over -5 to 0 seconds.

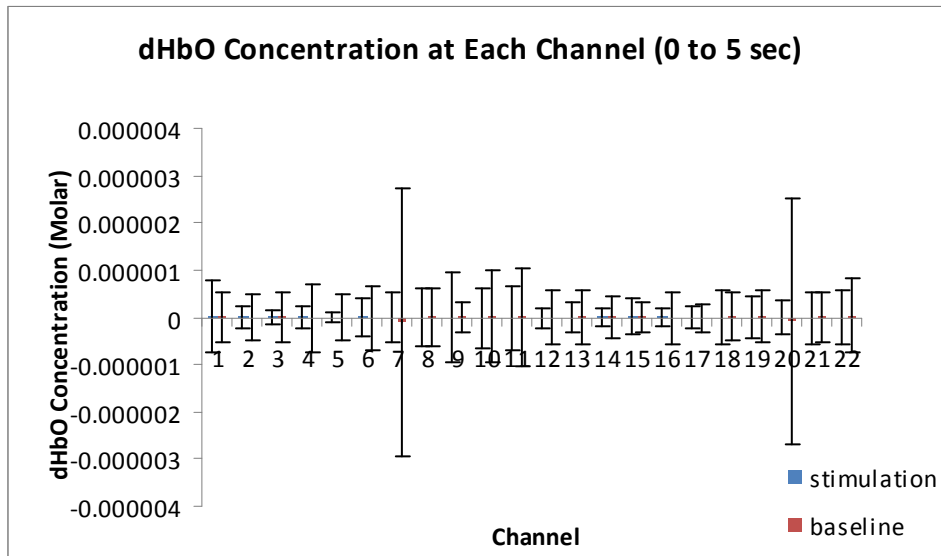


Figure B.7 Mean of the change in deoxygenated hemoglobin at each channel over 0 to 5 seconds.

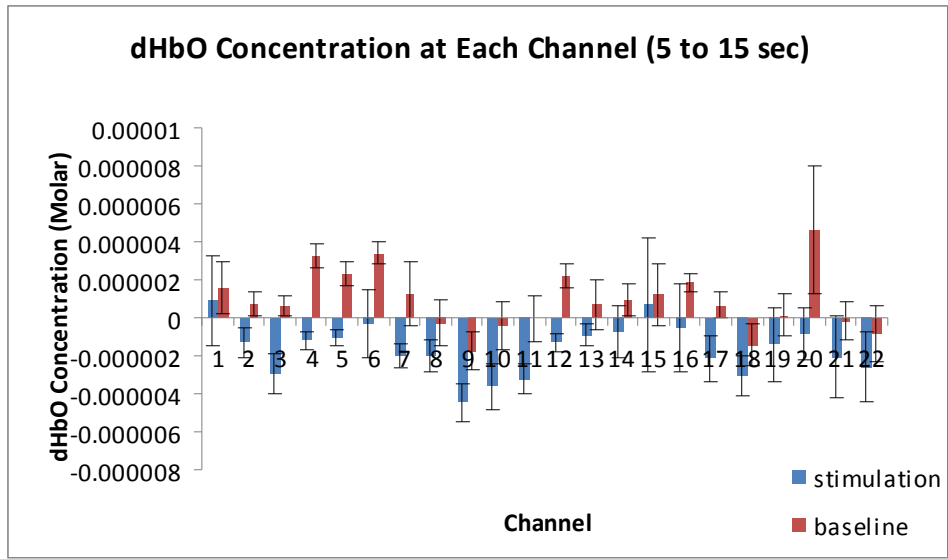


Figure B.8 Mean of the change in deoxygenated hemoglobin at each channel over 5 to 15 seconds.

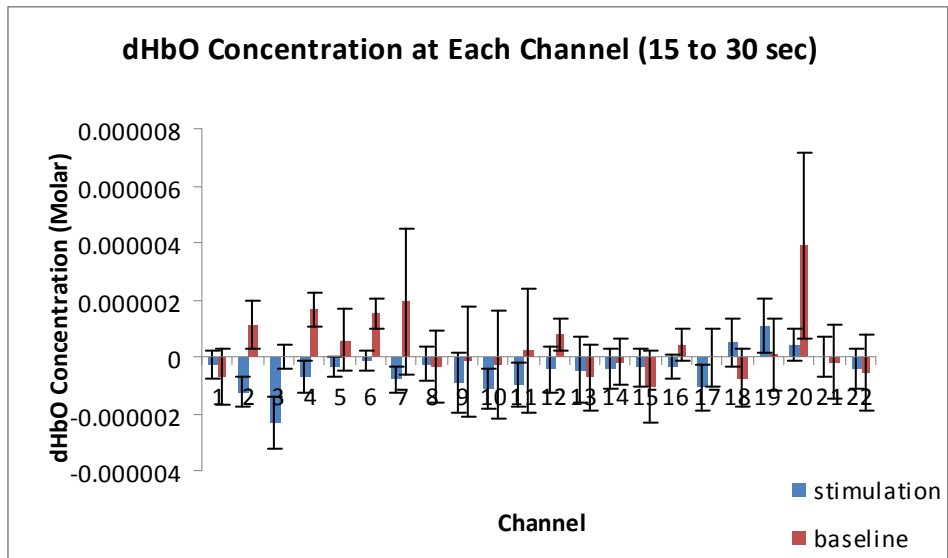


Figure B.9 Mean of the change in deoxygenated hemoglobin at each channel over 15 to 30 seconds.

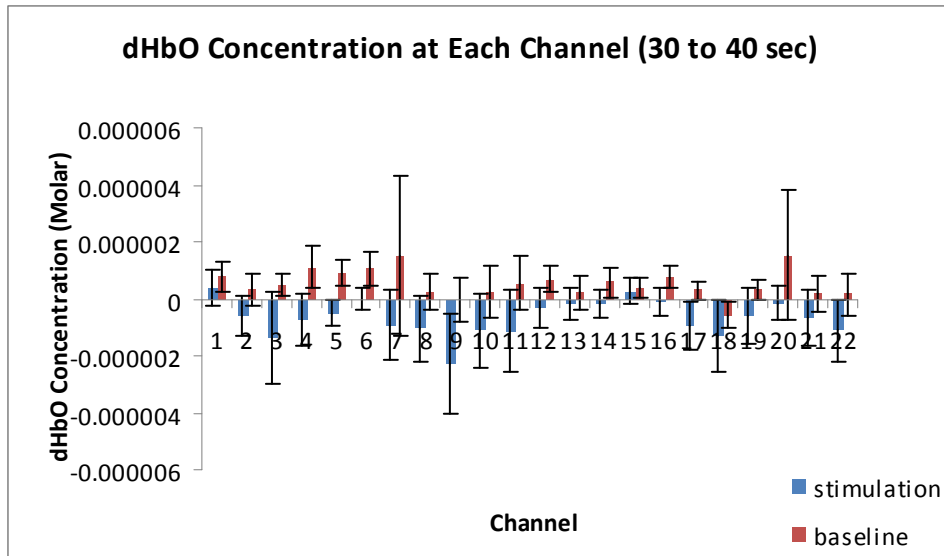


Figure B.10 Mean of the change in deoxygenated hemoglobin at each channel over 30 to 40 seconds.

REFERENCES

1. (29 November 2010). Pain. (Online), 15 October 2010. <http://en.wikipedia.org/wiki/Pain>
2. Tiengo, M., 2003. Pain perception, brain and consciousness. *Neurological Science* 24, S76-S79.
3. 2000. *Principles of Neural Science*, 4th Ed. E.R Kandel, J.H. Schwartz, T.M. Jessell (eds). New York: McGraw-Hill.
4. Tiengo M (1992) Nociception and pain: the brain and the mind, in *Highlights on Pain and Suffering*, Abstracts V. Ventafridda ed., Lugano, pp 11–12
5. Mayhew, J.E.W., 2003. Neuroscience: A measured look at neuronal oxygen consumption. *Science* 229, 1023-1024. 9 October 2010. <http://www.sciencemag.org/content/299/5609/1023.full>
6. Buxton, R.B., Uludag, K., Dubowitz, D. J., Liu, T. T., 2004. Modeling the hemodynamic response to brain activation. *NeuroImage* 23, S220-S233.
7. Schoedel, A.L. A., Zimmerman, K., Handwerker, H. O., Foster, C., 2008. The influence of simultaneous ratings on cortical BOLD effects during painful and nonpainful stimulation. *Pain* 135, 131-141.
8. Apkarian, A. V., Bushnell, M.C, Treede, R., Zubieta, J., 2005. Human brain mechanisms of pain perception and regulation in health and disease. *European Journal of Pain* 9, 463-484.
9. Stammer, T., De Col, R., Seifert, F., Maihofner, C. 2008. Functional imaging of sensory decline and gain induced by differential noxious stimulation. *NeuroImage* 42, 1151-1163.
10. Lopez-Sola, M., Pujol, J., Hernandez-Ribas, R., Harrison, B.J., Ortiz, H., Soriano-Mas, C., Deus, J., Mechon, J. M., Vallejo, J., Cardoner, N. 2010. Dynamic assessment of the right lateral frontal cortex response to pain stimulation. *NeuroImage* 50, 1177-1187

11. Bortfeld, H., Wruck, E., Boas, D.A. 2007. Assessing infants' cortical response to speech using near-infrared spectroscopy. *NeuroImage* 34, 407-415.
12. Sitaram, R., zhang, H. Guan, C., Thulasidas, M., Hoshi, Y., Iashikawa, A., Shimizu, K., Birdaumer, N., 2007. Temporary classification of multichannel near-infrared spectroscopy signals of motor imagery for developing a brain-computer interface. *NeuroImage* 34, 1416-1427.
13. TechEn. NIRSOptix (Online), 22 Nov 2010. <http://www.nirsOptix.com/CW6.html>
14. Bartocci, M., Bergquist, L. L., Lagercrantz, H., Anand, K.J.S, 2006. Pain activities cortical areas in the preterm newborn brain. *Pain* 122, 109-117.
15. Tachtsidis I., leung T.S., Devoto, L., Delpy, D.T., Elwell, C.E., 2008. Measurement of frontal lobe functional activation and related system effects: a near-infrared spectroscopy investigation. *Advances in Experimental Medicine and Biology* 614, 397-403.
16. Kohlloffel, L.U.E., Koltzenburg, M., Handwerker, H.O., 1991. A novel technique for the evaluation of mechanical pain and hyperalgesia. *Pain* 46, 81-87.
17. Koltzenburg, M., Handwerker, H. O., 1994. Differential ability of human cutaneous nociceptors to signal mechanical pain and to produce vasodilation. *Journal of Neuroscience* 14, 1756-1765.
18. Tian, F. Chance, B., Liu, H., 2009. Investigation of the prefrontal cortex in response to duration-variable anagram task using functional near-infrared spectroscopy. *Journal of Biomedical Optics* 14(5), 054016.
19. Tian, F., Sharma, V. Kozel, F.A., Liu, H., 2009. Functional near-infrared spectroscopy to investigate hemodynamic responses to deception in the prefrontal cortex. *Brain Research* 1301, 120-130.
20. Visual Analog Pain Scale. Figure, 11 November 2010. hubpages.com/hub/rating-the-pain

21. Lui, F., Duzzi, D., Carradini, M., Serafini, M. Baraldi, P., Porro, C.A., 2008. Touch or pain? Spatial-temporal patterns of cortical fMRI activity following brief mechanical stimuli. *Pain* 138, 362-374.
22. Hespos, S. J., 2010. What is Optical Imaging? *Journal of Cognition and Development* 11(1), 3 – 15.
<http://www.informaworld.com/smpp/section~db=all~content=a919239259~fulltext=713240928~dontcount=true>
23. Photom Migration Imaging Lab. HOMER (Online), 11 November 2010.
<http://www.nmr.mgh.harvard.edu/PMI/resources/homer/home.htm>
24. Bantick, S. J., Wise, R.G., Ploghaus, A., Clare, S., Smith, S.M., Tracey, I., 2002. Imaging how attention modulates pain in humans using functional MRI. *Brain* 125, 310-319.
25. Wiech, K., Ploner, M., Tracey, I., 2008a. Neurocognitive aspects of pain perception. *Trends in Cognitive Sciences* 12, 306-313.

BIOGRAPHICAL INFORMATION

Pamela Tebebi received a Bachelor of Engineering in Biomedical Engineering from Vanderbilt University in 2002. She enjoyed research and had been doing research since high school. After graduating she worked in a biomedical science research laboratory before joining corporate America in the pharmaceutical sector. While working, she decided to pursue a master's degree to further her education and career growth. During this time, she gained knowledge about current research topics and technological advancement in diagnostic and treatment tools. She obtained her Master of Science in Biomedical Engineering from the University of Texas at Arlington in 2011. Pamela plans on continuing her education to obtain a doctorate in engineering particularly in the area of clinical neuroengineering. Her goal is to develop tools that go from the engineering bench to the bedside of patients.